Producing Hollow Shafts in a New Horizontal Mill by Novel Flat-Knifing Cross-Wedge Rolling With Single Guide

Longfei Lin
University of Science and Technology Beijing https://orcid.org/0000-0001-5513-3829
Baoyu Wang (bywang@ustb.edu.cn)
University of Science and Technology Beijing
Jinxia Shen
University of Science and Technology Beijing
Tao Liu
University of Science and Technology Beijing

Research Article

Keywords: Flat-knifing cross-wedge rolling, Horizontal cross-wedge rolling mill, Multifunctional rolling mill, Single guide rolling, Hollow shafts rolling

Posted Date: June 3rd, 2021

DOI: https://doi.org/10.21203/rs.3.rs-569126/v1

Version of Record: A version of this preprint was published at The International Journal of Advanced Manufacturing Technology on October 3rd, 2021. See the published version at https://doi.org/10.1007/s00170-021-08023-0.

Producing hollow shafts in a new horizontal mill by novel flat-knifing cross-wedge rolling with single guide

Longfei Lin [a], Baoyu Wang [a,b*], Jinxia Shen [a], Tao Liu [a]

[a] School of Mechanical Engineering, University of Science and Technology Beijing, Beijing 100083, China

[b] Beijing Laboratory of Metallic Materials and Processing for Modern Transportation, Beijing 100083, China

* Corresponding author: Baoyu Wang

E-mail address: bywang@ustb.edu.cn

Tel: +86-010-82375671

Fax: +86-010-82375671

Postal address: No.30 Xueyuan Road, Haidian District, Beijing 100083, China

Abstract

To meet the requirement of lightweight, there are increasing solid shafts being designed to be hollow in transportation industry. In this study, a novel method of flat-knifing cross-wedge rolling (FCWR) with single guide is proposed including a modified roller, a horizontal mill and a single-guide structure, and its key problems are studied by numerical simulations and experimental tests. A mathematical model of FCWR roller is established, which reveals the wedge length of rollers is effectively reduced by modifying knifing wedge from normalized roller. Further, a horizontal multifunctional mill is invented and constructed to carry out the FCWR experiment with single guide. According to the results from the numerical simulations and corresponding experiments, it is observed that the typical defects of hole expansion and knifing groove are absolutely avoided because the improved flat-knifing wedge produces a radial force to shrink the inner hole and avoid the deformation concentration of the outer surface during knifing stage. Moreover, the single guide rolling performed in the horizontal mill efficiently improve rolling stability because the workpiece is restricted into a smaller workspace. To the authors' knowledge, all these integrated improvements of FCWR roller, single guide rolling and horizontal mill are innovative, which are of great engineering significance to manufacture hollow shafts on account of the advantages of avoiding forming defect, reducing roller diameter, improving rolling stability and simplifying mill structure.

Keywords: Flat-knifing cross-wedge rolling; Horizontal cross-wedge rolling mill; Multifunctional rolling mill; Single guide rolling; Hollow shafts rolling

Nomenclature

α	Forming angle
β	Stretching angle
B	Knifing width
L	Sizing width
η	Workpiece reduction
h	Wedge height
d_m	Mandrel diameter
D_0, d_0	Outer and inner diameter of workpiece before rolling
D_1, d_1	Outer and inner diameter of workpiece after rolling
L_{N1}, L_{F1}	Knifing length of NCWR wedge and FCWR wedge
L_{N2}, L_{F2}	Stretching length of NCWR wedge and FCWR wedge
L_{N3}, L_{F3}	Sizing length of NCWR wedge and FCWR wedge
L_R	Wedge length reduction from NCWR to FCWR

1 Introduction

Since hollow shafts have advantages of lightweight structure, low rotating inertia and convenient flaw detection, more and more solid parts are designed to be hollow such as railway axles [1], engine valves [2], and truck shafts [3]. Up to now, these hollow shafts are mainly formed by forging, extrusion and drilling, which result in the waste of material and low production efficiency.

Cross wedge rolling (CWR), a near-net shape metal manufacturing process with high production efficiency and low material consumption, has an extensive application in solid shafts including large-elongated parts (e.g., automobile camshafts, stepped shafts) and die-forging preforms (e.g., engine valves, connecting rods, double-ended spanners) as reviewed by Hu et al. [4] and Pater et al. [5]. Hu et al. [4] pointed out they have established more than 300 production lines worldwide with an estimated production value of more than $200 million per year, and highlighted that the weight of CWR products has over 400,000 tons with an amount of 2 billion pieces per year in China. However, although CWR has been successfully used on solid shafts, it is less common on hollow shafts.

Compared with forging, extrusion and drilling process, CWR of hollow shafts has advantages of high efficiency, not need lubricant and less loading. Researchers have been concerned about its applications. Huo et al. [6] presented a CWR process for high-speed railway axles, and predicted the microstructure and ductile damage at hot forming. Ji et al. [2] proposed to manufacture hollow valve-preforms by CWR, and investigated the influence of process parameters. Yang et al. [3] developed a process of CWR hollow axle sleeve, and studied the elliptical behavior of inner hole. Pater et al. [7] presented a conception of the three-roller cross rolling process of hollow rail axles, and found that the walls of formed steps are thickened. Peng et al. [8] used a multi-wedge CWR without mandrel to produce hollow high-speed railway axle, and reached a conclusion that the double-wedge CWR for large and long thick-walled hollow shafts is feasible. These works are meaningful and have pointed out a new approach to manufacture

hollow shafts.

To establish a reliable technique for rolling hollow shaft, CWR without mandrel was early proposed and investigated. Bartnicki and Pater [9, 10] analyzed the numerical simulation results and found the thinner wall thickness may cause the slipping and flattening of billet, and concluded the three-roller CWR can improve rotation conditions. Urankar et al. [11] proposed a dimensionless crushing parameter to predict forming limit of the hollow products, and the defect of hole expansion was shown in their study. However, CWR without a mandrel has a common shortcoming that its inner hole is unable to be regularly formed because the hole is formed randomly.

A process of CWR with mandrel was proposed to control the dimensions of inner hole, and researches have been done to improve its forming performance. Neugebauer et al. [12] proposed two ways to control the movements of mandrel: fixed or freedom mandrel. Landgrebe et al. [13] modified the typical CWR via adding a drilling mandrel, therefore a hollow shaft can be directly rolled from a solid billet. Shen et al. [14, 15] used a compensated mandrel to produce hollow shafts with a variable inner diameter. Recently, Shen et al. [16] based on the volume consistency principle, and established a theoretical model to predict the critical mandrel diameter. However, many of these researches have focused on mandrel design and parameter optimization, but pay less attention to roller modification.

In normalized CWR with mandrel, as shown in Fig.1, although inner hole can be controlled, it brings about the defects of hole expansion and knifing groove [17-20]. Hole expansion exists on the inner hole, while knifing groove on the outer surface. These defects reduce the utilization of materials and increase the cost of post-processing. Ji et al. [17] employed variable stretching angle to avoid hole expansion, but make roller design complicated. In engineering practice, skilled workers generally solve the hole expansion by chamfering knifing-wedge. Actually, both hole expansion and knifing groove occur in the knifing position of rolled shafts. Therefore, modifying the shape of roller on knifing zone is of great significance.

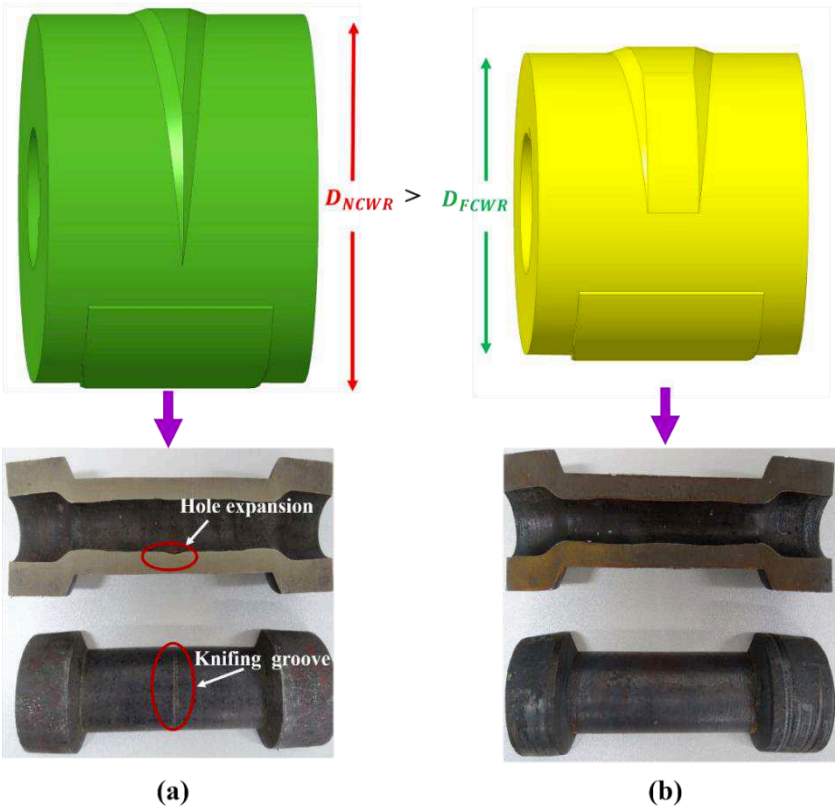

Fig. 1 Contrast between two methods for hollow shafts：(a) normalized CWR; (b) flat-knifing CWR

In this study, a novel flat-knifing cross-wedge rolling (FCWR) with single guide for hollow shafts (Fig.1b) is proposed whereby modifying roller and mill from the base of normalized cross-wedge rolling (NCWR), which takes advantages of avoiding the defects of hole expansion and knifing groove, reducing the diameter of rollers, improving rolling stability and simplifying mill structure.

In order to study the new process systematically, its key points are investigated by numerical simulation and experimental research. Firstly, the new process of FCWR with single guide is described in detail. Secondly, the mathematical model of FCWR roller is established and the length reduction is calculated and visually presented. Thirdly, numerical simulations are conducted to compare the NCWR and FCWR process from the aspects of defect formation mechanisms, workpiece deformation characteristics and influences of new parameter. At last, corresponding physical FCWR experiments are performed to verify the FE results, and the advantages and disadvantages of these improvements are discussed.

2 Flat-knifing cross-wedge rolling with single guide

2.1 Novel process principle

The process principles of normalized cross-wedge rolling (NCWR) with two guides and flat-knifing cross-wedge rolling (FCWR) with single guide are shown in Fig. 2. They have same deform mechanism that a cylindrical hollow billet is deformed into a stepped hollow shaft under the action of roller whereby wedged rollers moving tangentially relative to each other.

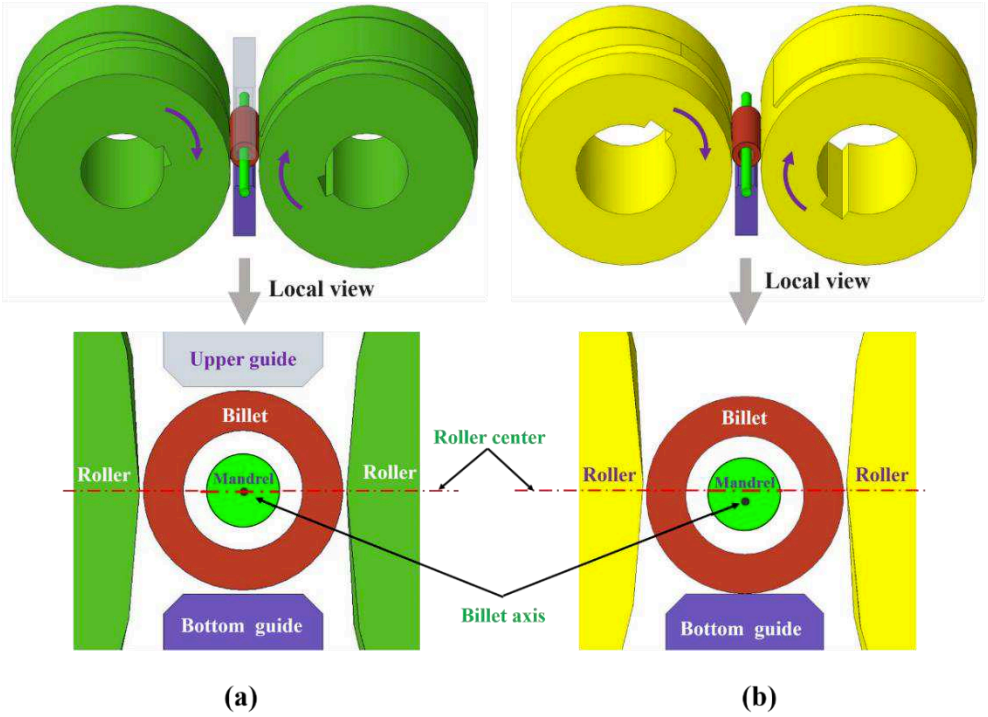

Fig. 2 Process principle: (a) NCWR with two guides; (b) FCWR with single guide

There are some improvements: 1) the knifing wedge of FCWR roller is flatted, while that of NCWR is sharped; 2) differing from NCWR has a vertical structure, FCWR process changes into a horizontal arrangement that can achieve single guide rolling under gravity; 3) by single guide rolling, FCWR workpiece is steadily restricted into a smaller workspace. As a result, the novel process is estimated has advantages of:

- the defects of hole expansion and knifing groove can be absolutely avoided;
- the diameter of two rollers can be evidently shortened;
- the mill can be simplified into single guide structure;
- The rolling stability can be improved.

2.2 New type of horizontal multifunctional mill

In order to achieve the technical objective of single guide rolling, a laboratory mill with a horizontal structure is indispensable. Up to now, the traditional CWR mills commonly have a vertical structure [4, 5, 22], which apparently cannot meet the requirement of this study.

Therefore, a new type of rolling mill is invented and constructed by the authors [23]. The freedoms of this mill has been increased by two angle adjusting systems, one radial feeding system, and a synchronous unit (worked by two matched gears). Its 3D model is shown in Fig. 3, the mill is presented in Fig. 4, and the technical specifications are given in Table. 1.

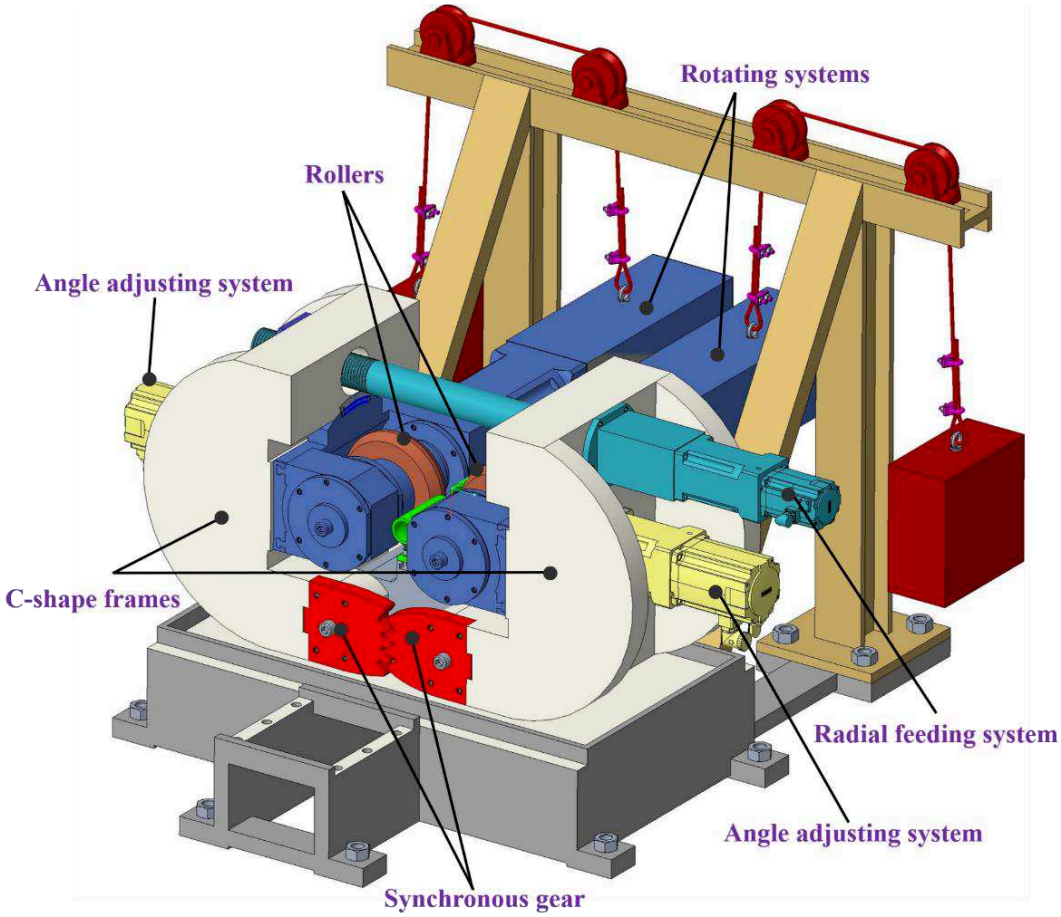

Fig. 3 Geometrical model of the horizontal multifunctional mill [23]

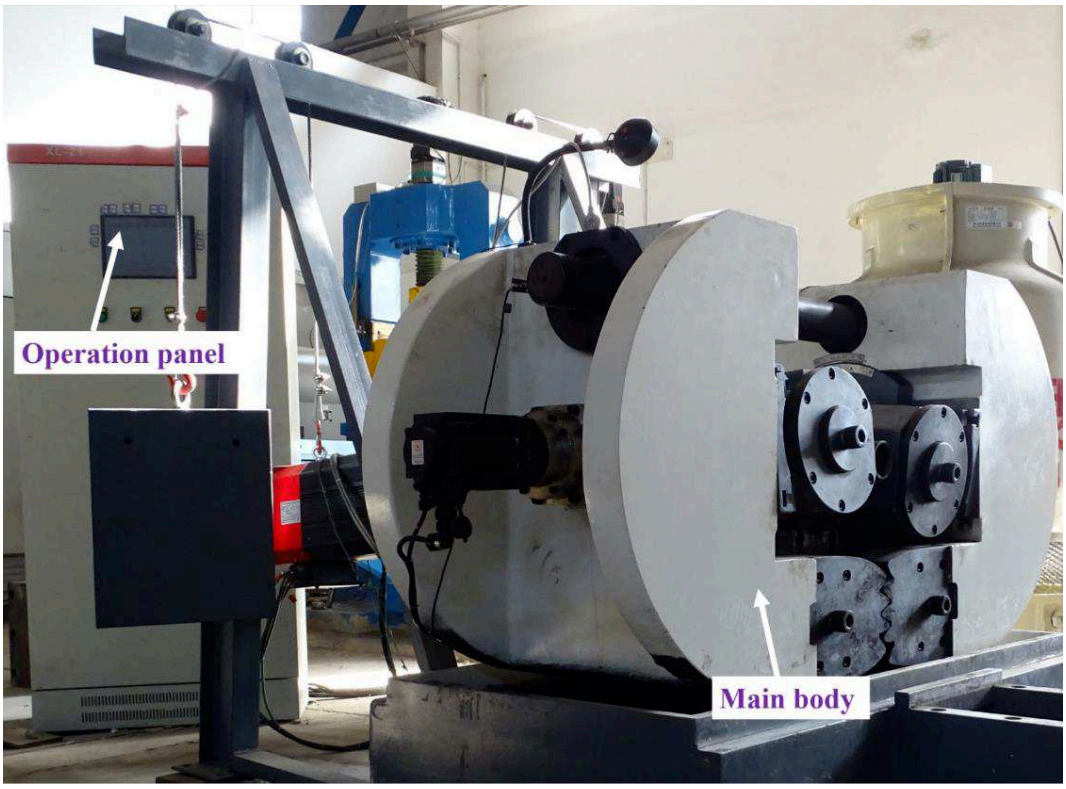

Fig. 4 The constructed horizontal multifunctional mill [23]

Table 1 Technical specifications of the horizontal multifunctional mill

Parameter	Unit	Value
Power of main rotating motor	kW	2×30
Speed of main rotating	rpm	0~43
Power of Radial feeding motor	kW	3
Speed of Radial feeding	mm/s	1~5
Power of angle adjusting motor	kW	2×2.3
Speed of angle adjusting	°/s	1~10
Range of angle adjusting	°	±12
Maximum diameter of roller	mm	350
Maximum diameter of billet	mm	80
Overall dimensions	m	1.8×1.7×1.6
Total power	kW	70
Total weight	ton	5

This mill is characteristic of multiple freedom degree because has several movements of circumferential rotating, radial feeding and angle adjusting, and thus it can be used for different types of laboratory rolling tests such as longitudinal rolling, cross rolling, and skew rolling.

All the motions of this mill are directly driven by servo motors that mill structure is compact. As signed in Fig.3, two C-type frames are used to enchence mill strength, the automation system is controlled by a accurate servo drive which programed in PLC language. All these features may take this type of mill advantages of compact structure, high strength and high precision, so that it can be expected to be industrially applied as thread rolling mill, ball rolling mill and CWR mill.

2.3 New type of flat-knifing roller

Roller modification is a main innovation of this paper. In the hope of mathematically describing the FCWR roller in detail, both the geometrical models of FCWR and NCWR roller are designed and shown in Fig. 5 with a plane layout way.

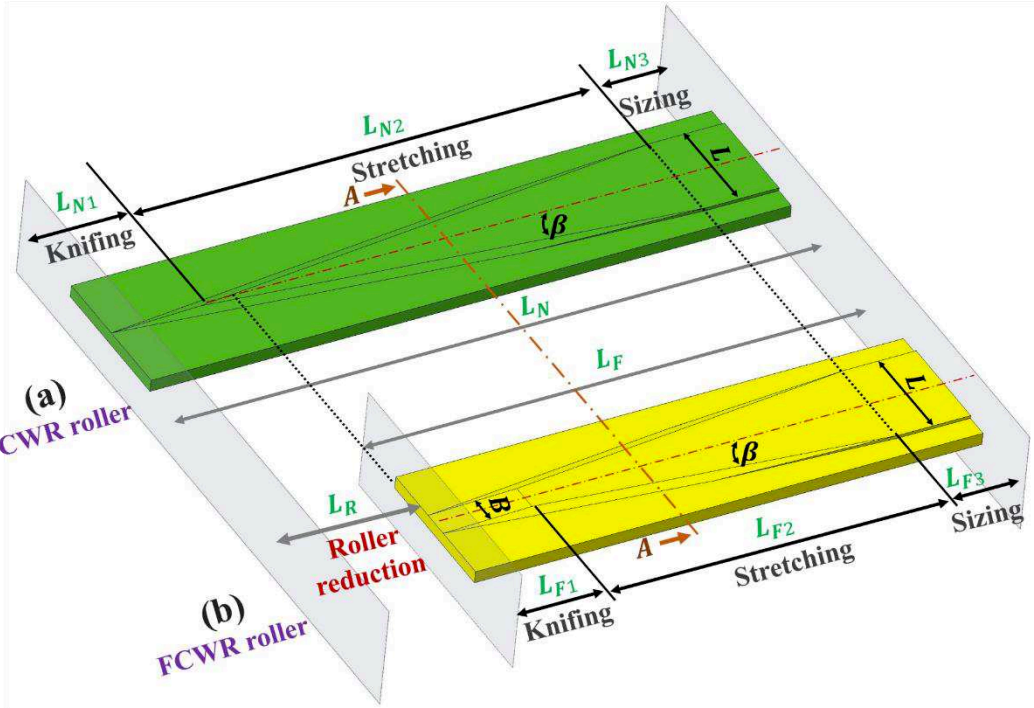

Fig. 5 Configuration and major parameters of NCWR and FCWR roller

There is an obvious difference observed in the figure that the knifing zone of NCWR roller is designed as a V-shaped wedge, while FCWR roller is a flat-wedge with

a width of B. Further, the FCWR roller only changes the wedge shape in the knifing zone, and their configurations are identically divided into three sections as knifing zone, stretching zone and sizing zone. Fig. 6 shows that their contact models (extracted from the A-A view of Fig. 5) between roller, mandrel and workpiece of FCWR and NCWR roller are exactly same on stretching zone. To make an analysis, on the one hand, the main deformation of FCWR rolling is occurred in stretching zone, where FCWR has the same contact model with NCWR. On the other hand, FCWR process have the same sizing zone with NCWR. As a conclusion, these modifications have not changed the process parameters form the NCWR, so that both NCWR and FCWR may have the same process parameters such as forming angle α, stretching angle β and mandrel diameter d_m.

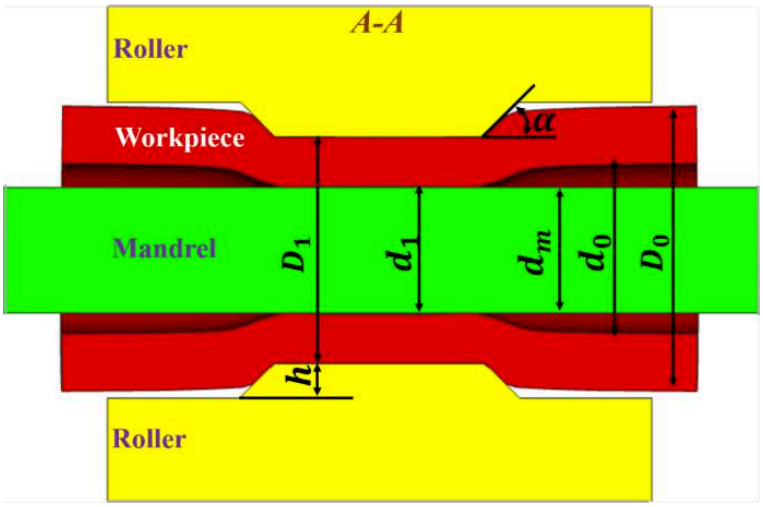

Fig. 6 Contact model of roller, mandrel and workpiece at the stretching stage

In order to mathematically compare FCWR and NCWR roller, the calculation of wedge length is a basic work, which need to be undertaken primarily.

At the knifing zone, notwithstanding the different geometries, the wedge lengths of FCWR and NCWR roller are equally formulated as Eq. 1, where h is the height of wedge, α is forming angle, and β is the stretching angle.

$$L_{N1} = L_{F1} = h \cot\alpha \cot\beta \tag{1}$$

At the stretching zone, because the initial position of FCWR wedge have a straight section, L_{N2} is obviously longer than L_{F2}, and they are respectively calculated by Eq. 2

and Eq. 3, where L represents the sizing width (signed in Fig. 5) and B represents the knifing width.

$$L_{N2} = 0.5L\cot\beta \tag{2}$$

$$L_{F2} = 0.5(L-B)\cot\beta \tag{3}$$

Owing to the geometries at sizing zone of NCWR and FCWR are exactly same, they have same sizing length which can be formulated by Eq. 4, where D_0 and D_1 are the outer diameter of the workpiece before and after rolling.

$$L_{N3} = L_{F3} > 0.25\pi(D_0+D_1) \tag{4}$$

Because the length of each zone is determined through the above equations, the length reduction L_R can be calculated by Eq. 5.

$$L_R = 0.5B\cot\beta \tag{5}$$

For a purpose of a more intuitive comparison of the wedge length of roller, their formulas are summarized in Table 2. It can be concluded that the lengths of knifing wedge and sizing wedge of NCWR and FCWR roller are equal in value, while FCWR stretching length is shorter than that of NCWR.

Table 2 Mathematical comparison of the wedge lengths of NCWR and FCWR roller

Type	NCWR	FCWR	Comparison
Equation	$L_{N1} = h\cot\alpha\cot\beta$	$L_{F1} = h\cot\alpha\cot\beta$	$L_{N1} = L_{F1}$
	$L_{N2} = 0.5L\cot\beta$	$L_{F2} = 0.5(L-B)\cot\beta$	$L_{N2} > L_{F2}$
	$L_{N3} = 0.25\pi(D_0+D_1)$	$L_{F3} > 0.25\pi(D_0+D_1)$	$L_{N3} = L_{F3}$
Length reduction	$L_R = 0.5B\cot\beta$		

In order to visually reveal the relationship between wedge-length reduction and process parameters, a three-dimensional graphic have been drawn as expressed in Fig. 7. The length reduction L_R is only related to stretching angle β and knifing width B, which increases with the increase of B and β in range of 200~800mm. Take an example of the roller used in the experiment of later study: β=2 °, B=18 mm, its wedge length

reduction reaches up to 257.7 mm.

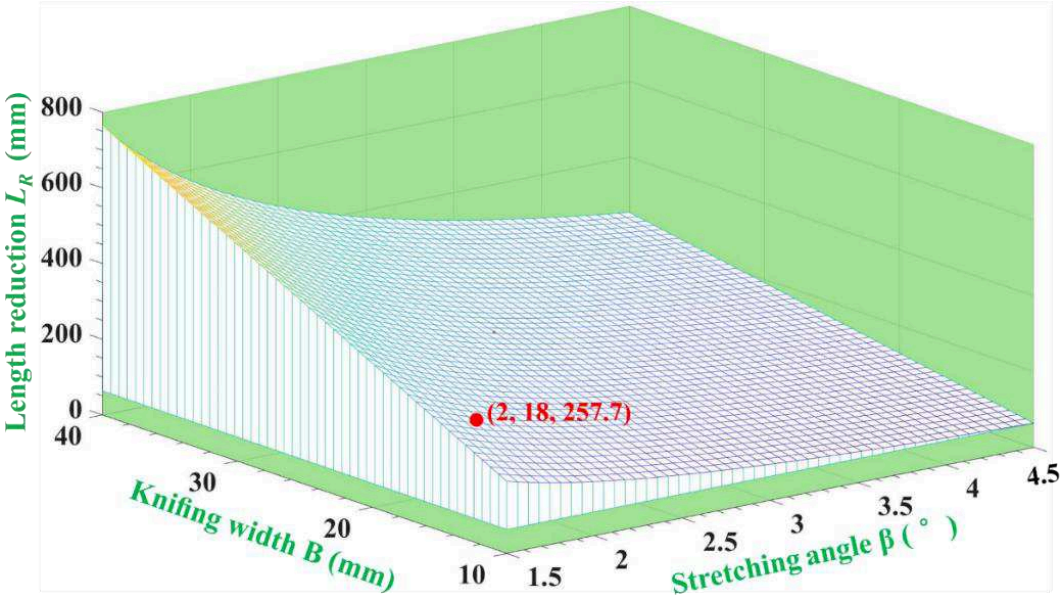

Fig. 7 Relationship between wedge-length reduction and process parameters

3 Parameter ranges and research schemes

Considering process parameters will directly affect whether this novel process is successful or not, the ranges of major parameters are discussed and summarized based on the previous research of NCWR hollow shafts [16, 17, 24].

(1) The workpiece reduction η. Workpiece reduction reflects deformation degree and the flattening of workpiece. In the case of hollow billet with thin wall, the large η make the rolling piece undergo serious flattening deformation and then the rolling status is instability, so that the products become elliptical finally. In addition, when the hollow billet has a thick wall, in this case the rolled piece has a better resistance to flattening deformation, the roundness of the rolled products is improved under the condition of a larger η because of the good flow of axial metal. The workpiece reduction η is expressed and ranged as Eq. 6.

$$0.2 < \eta = \frac{D_0 - D_1}{D_0} < 0.4 \tag{6}$$

(2) The forming angle α. Forming angle is an important roller parameter, which directly determines the contact surface of of forming area and then affects the metal

flow. In the reason that hollow billet is more prone to elliptical and then the axial flow of the metal may become worse, the forming angle of the hollow shafts rolling is generally greater than that of solid shafts, whose value is usually derived as follows：

$$30\ ^\circ<\alpha<50\ ^\circ \tag{7}$$

(3) The stretching angle β. Stretching angle is another important tool parameter. Increasing its value is beneficial to decrease the length of roller but enlarges the tangential deformation of the workpiece, as a result, it is easy to cause oval deformation. Therefore, the stretching angle for hollow shafts is generally smaller than solid shafts, its range is：

$$1.5\ ^\circ<\beta<4.5\ ^\circ \tag{8}$$

(4) The mandrel diameter d_m. The mandrel is used to control the shapes and dimensions of inner hole. When its diameter is too small, mandrel will unable to contact inner hole and out of service. And when its value gets too large, it makes the rolling wall thin seriously and wall deformation become severe, thus billet cannot rotate normally. Its value is usually designed as Eq. 9, in which d_0 is the initial diameter of inner hole.

$$0.5d_0<d_m<0.9d_0 \tag{9}$$

(5) The knifing width B. Knifing width is a new parameter which only exists on FCWR roller. On the basis of previous explorations (discussed in later sections), larger knifing width allow for less length of wedge but increase workpiece ellipticity, rolling force, and rotating torque. Its value is generally selected as:

$$10\ \text{mm}<B<40\ \text{mm} \tag{10}$$

On the basis that the selection ranges of main parameters have been determined, a research scheme combined FE simulations and experimental tests has been worked out as demonstrated in Table 3. The FE simulation is adopted to compare the distinction on NCWR and FCWR from the aspects of defect mechanisms, deformation characteristics and influences of new parameter. Correspondingly, the physical FCWR tests are conducted to verify the FE results and reveal the advantages and disadvantages of

279 FCWR process.

280 **Table 3.** Research schemes and parameter values

Parameter symbol (unit)	Billet inner diameter d_0 (mm)	Mandrel diameter d_m (mm)	Knifing width B (mm)	Method
NCWR	30	none	none	FE
	30	22	none	FE
FCWR	30	none	18	FE, Test
	30	22	14, 18, 22	FE
	30, 28, 26, 24	22, 20.5, 19, 17.6	18	Test

281 Besides, D_0=50 mm, α =45 °, β=2°, h=6 mm, T=1050 °C, d_m/d_0=0.73.

282 **4 Numerical simulations of NCWR and FCWR with single guide**

283 **4.1 Finite element modeling**

284 Preliminary feasibility study was done by numerical simulations. Both NCWR and
285 FCWR finite element (FE) models were established. It should be pointed out that, the
286 FE model of NCWR and FCWR only changed the rollers while other parameters such
287 as billet dimensions, rolling temperature and mandrel dimensions stayed the same. The
288 FE scheme and parameter were carried out according to Table 3.

289 The FE projects were performed in Simufact.Forming software, which has been
290 successfully employed in numerical analysis of CWR process [25, 26] and skew rolling
291 process [27, 28], and their FE results have a good agreement with experimental results.
292 The FE projects of NCWR and FCWR with single guide were modeled as Fig. 8 shows.
293 Both the geometric models of NCWR and FCWR were consisted of two rollers, one
294 guide, one mandrel and one workpiece. The positional relationships between each part
295 were set up as marked in Fig. 2. The workpiece axis was downwardly offset from roller
296 centre with a 3 mm distance.

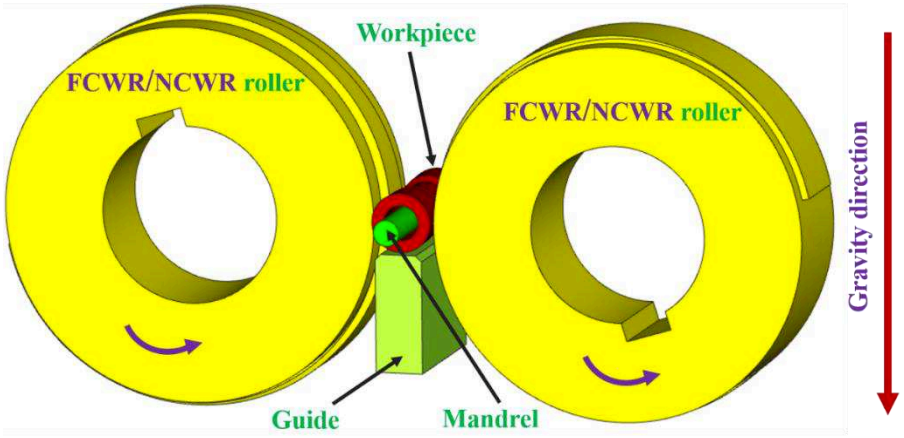

Fig. 8. FE projects of FCWR and NCWR with single guide.

The billet is C45 steel rod with an outer diameter of 50 mm, an inner diameter of 30 mm and a length of 100 mm. Its material data were taken from Simufact.Material. The properties (i.e., density, Young's modulus and Poisson's ratio) were set as default. The flow stress of C45 steel was defined by Eq. 11, in which σ_F is the flow stress (MPa), φ is the eff ective strain (-) and T is the temperature (°C):

$$\sigma_F = 2589.85e^{-0.003125T}\varphi^{(0.00004466T-0.10127)}e^{(-0.000027T+0.0008183)/\varphi}\dot{\varphi}^{(0.00015T-0.002749)} \quad (11)$$

The friction coefficients between tools and workpiece were modeled by Shear model (two rollers were 0.8, guide and mandrel were 0.2. [28] The temperature of tools (rollers, guide and mandrel) was constantly maintained at 300 °C [28]. The initial temperature of workpiece was 1050 °C and the coefficient of heat transfer between tools and workpiece was 10 kW/m^{2}K [28]. Besides, the mesh of billet was created by ringmesh mesher, whose element size equals to 1.4 mm, and will be automatically reconstruected if the eff ective strain increases by 0.4 [28]. Both the NCWR and FCWR rollers rotated at a same speed of 6 rpm.

4.2 Comparison of forming defects

Four FE results with the parameters of D_0=50 mm, d_0=30 mm, α=45 °, β=2 °, d_m=22 mm and B=18 mm was extracted from the software postprocessor and shown in Fig. 9. With the help of the numerical simulation, the shape of rolling workpiece can be acquired at every moment.

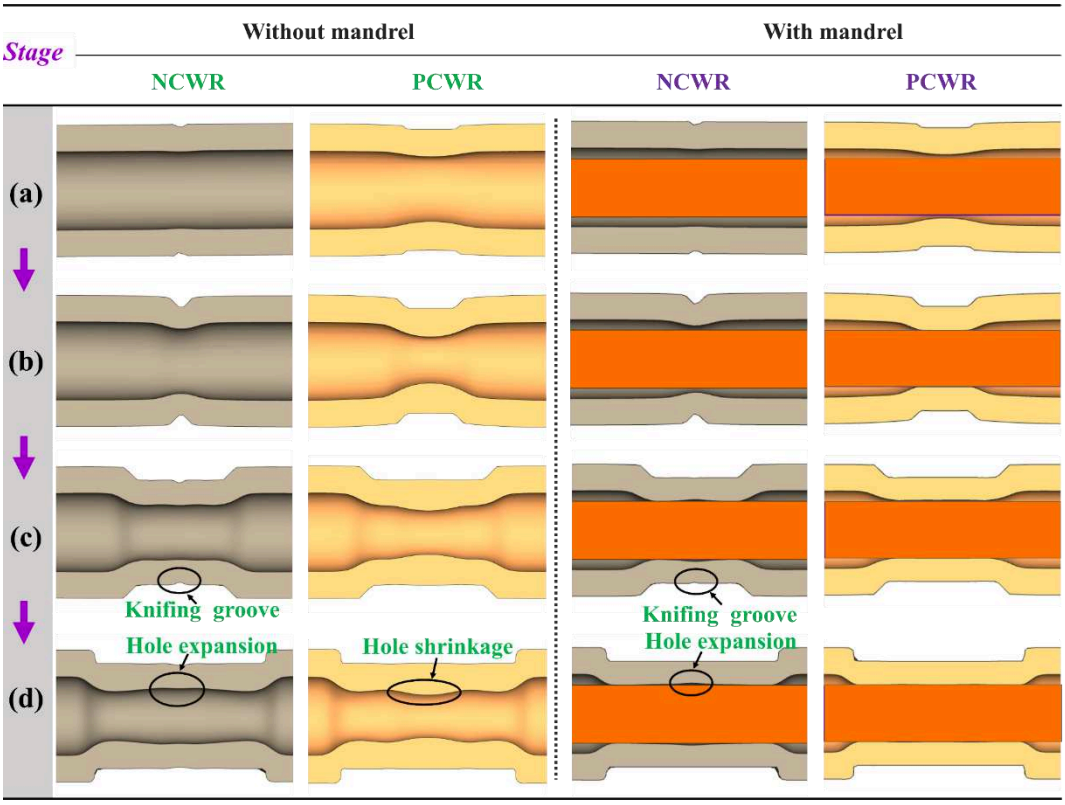

317 **Fig. 9** FE results of NCWR and FCWR: (a) middle of knifing stage; (b) end of knifing
318 stage; (c) middle of stretching stage; (d) end of stretching stage

319 At the middle of knifing stage, all the workpieces are not contact with mandrel.
320 But at the end of knifing stage, there is a difference that FCWR workpiece contacts with
321 mandrel while NCWR does not. Considering the values of mandrel diameters are the
322 same, it can be concluded that, the radial deformation of inner hole in FCWR process
323 is more serious than that in NCWR during the whole knifing stage.

324 The defects of hole expansion and knifing groove primitively appear on the
325 NCWR shafts at the middle of stretching stage regardless of whether it has mandrel or
326 not (Fig.9c). But in the case of FCWR shafts at this stage, these defects are completely
327 absent. Inversely, there is a hole shrinkage on the FCWR shaft without mandrel. As a
328 result, we can get the FE conclusion that: 1) no matter with or without mandrel, NCWR
329 rolled shafts universally have the defects of hole expansion and knifing groove; 2)
330 FCWR process without mandrel have a defect of hole shrinkage; 3) the FCWR process
331 with mandrel has a good geometric accuracy on outer and inner surface. The conclusion
332 optimistically verifies the technological assumptions, as a result, the FCWR with

mandrel was adopted on hollow shafts forming in later studies.

4.2.1 Hole expansion

Since hole expansion is a major defect in this study, it is necessary to reveal its formation mechanism from aspects of contact surface, loading states and the shape of inner hole (Fig. 10).

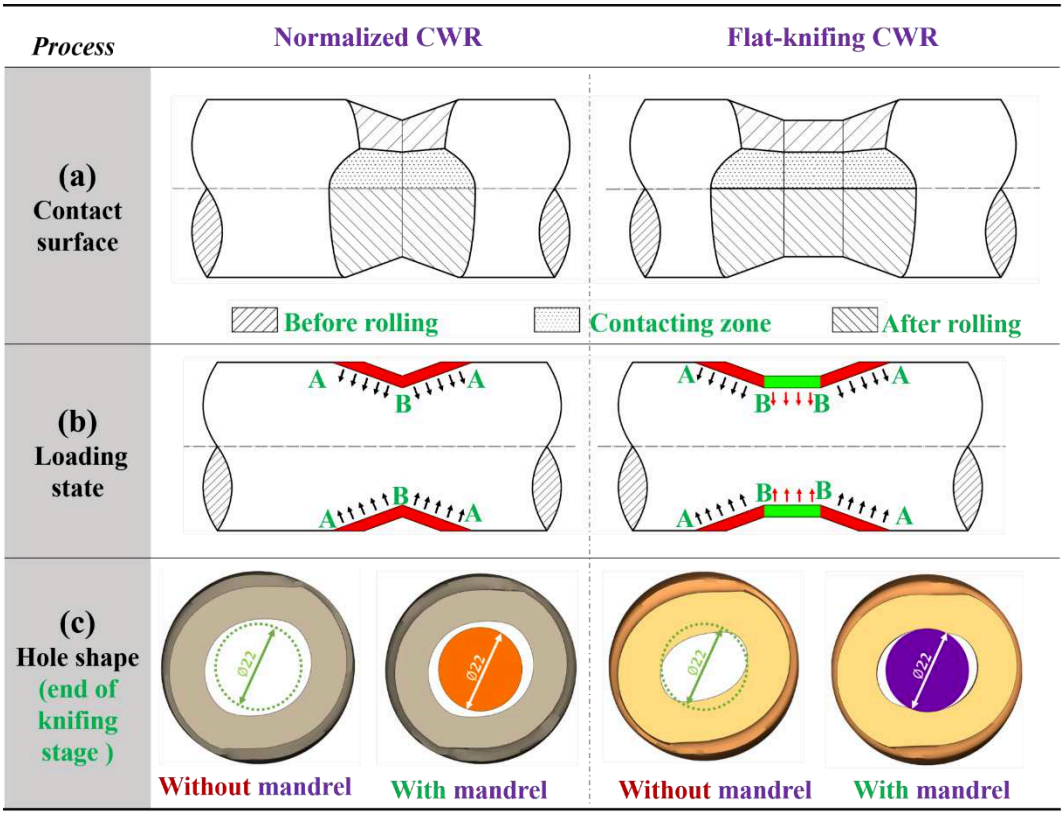

Fig. 10 Formation mechanism of hole expansion (end of knifing stage): (a) contact surface; (b) loading states; (c) hole shape

The contact surface of workpiece was drawn by Boolean subtraction operation in CAD software, which has indicated the different of deformation morphology between NCWR and FCWR. As shown the Fig. 10a, under the same forming angle α and stretching angle β, the main difference between NCWR and FCWR contact surface is that there is a rectangle contacting zone on the middle of FCWR workpiece.

Based on the drawn contact surface, the loading states can be acquired as Fig. 10b shows. At the NCWR knifing stage, because AB and BA segments individually produce a axial component on the side of knifing position, the inner hole is tensioned in axial

direction and then expanded radially. But in FCWR process, the added BB segment provides a radial force during the knifing stage that promotes the radial flow of the metal, and thus the inner hole is shrunk. Eventually, FCWR hole contacts with the mandrel while NCWR does not (Fig. 10c).

In short, FCWR process has an added radial force during knifing stage, which is helpful to the radial flow of the metal and then shrink the inner hole, so that the defect of hole expansion can be avoided in principle.

4.2.2 Knifing groove

Another defect concerned about in this study is the knifing groove, which typically appears on the CWR shafts regardless of whether they are hollow or solid [18, 19]. According to engineering practice, this defect can be avoided via chamfering the knifing-wedge. Obviously, this method cannot solve this defect at design stage. The geometric appearances of NCWR and FCWR workpiece are compared in Fig. 11.

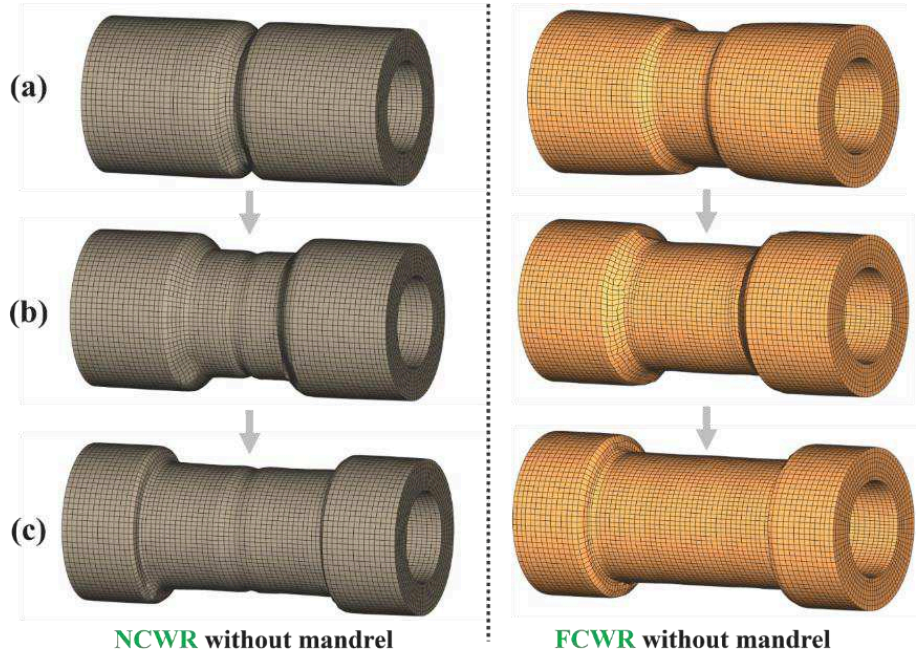

Fig. 11 Geometry comparison between NCWR and FCWR workpiece: (a) end of knifing stage; (b) middle of stretching stage; (c) end of stretching stage

The knifing groove initially appears on the NCWR shaft at the end of knifing stage and then remains until the end. It can be explained that deformation concentration exists on NCWR knifing area which makes the metal of surface undergo a severe local

deformation. As a result, a groove appears on the knifing position. When it comes to stretching and sizing stage, this defect is hard to be resolved because the height of wedge is constant. In the FCWR process, there is a flat segment BB existing on the middle as Fig. 10b shows, which can avoid the concentrated deformation that the defect of knifing groove does not appeared fundamentally.

4.3 Effect of new parameter

4.3.1 Hole ovality

The novel process introduces a new process parameter named knifing width *B*. Since it has an influence on the ovality of inner hole, an observation section selected from the axial centre of the workpiece are contrastively compared in Fig 12, which demonstrates that, as the knifing width *B* increases, the ovalization of inner hole becomes serious.

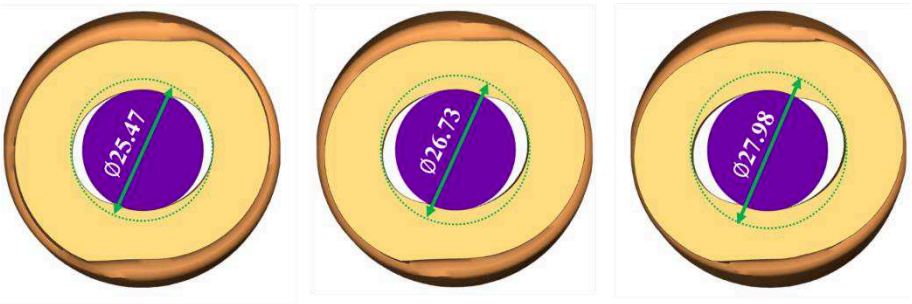

Fig. 12 Relationship between knifing width and hole ovality (end of knifing stage)

The ovality of inner hole has negative effect on rolling stability. When the ovality of inner hole is too large, the radial deformation of workpiece will be unstable. Under this situation, even if rollers are rotating normally, the slipped billet cannot rotate regularly. Hence, considering elliptical hole is bad for rolling stability, the value of knifing width should not be too large.

4.3.2 Rolling force and rotating torque

Rolling force in the radial direction and rotating torque are the basic data of rolling equipment, which directly determine the capacity of mill and can be predicted by FE

results as shown in Fig. 13.

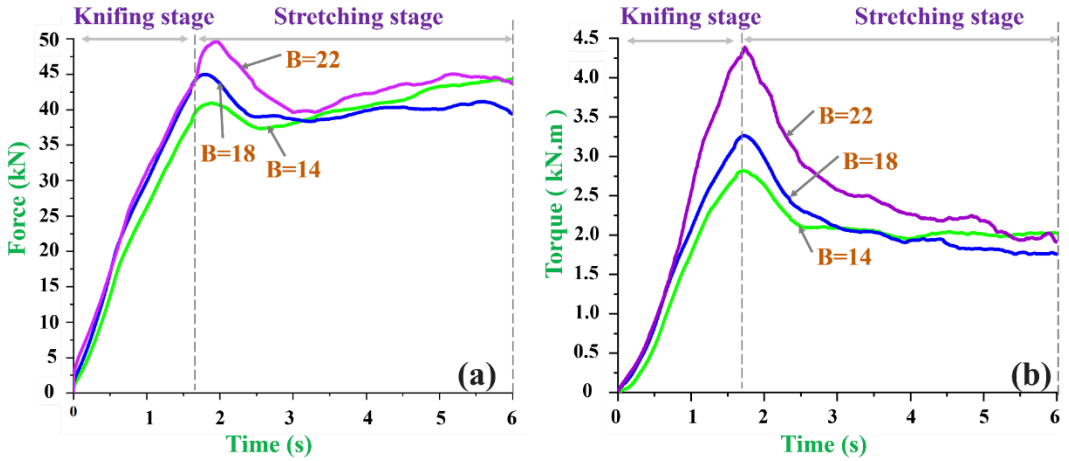

Fig. 13 Relationship between knifing width, (a) rolling force, and (b) rotating torque

The trends of rolling force and rotating torque are similar. Both rolling force and rotating torque gradually increase at the knifing stage and then decrease at the beginning of stretching stage. The maximum values of rolling force and rotating torque concurrently appear at the end of knifing stage. Significantly, the knifing width has an effect on the maximum values of rolling force and rotating torque. With knifing width *B* increases, the maximums of rolling force and rotating torque rise as well.

Based on above analysis, it can be concluded that large knifing width deteriorates the ellipse of hole and increases rolling force and rotating torque.

4.4 Formation of the inner hole

The formation of inner hole is a critical problem of hollow shafts rolling, which directly influences the forming accuracy and the rolled-wall performance. A cross-section is selected from the axial center of workpiece and observed at different rolling stages as Fig. 14 shows.

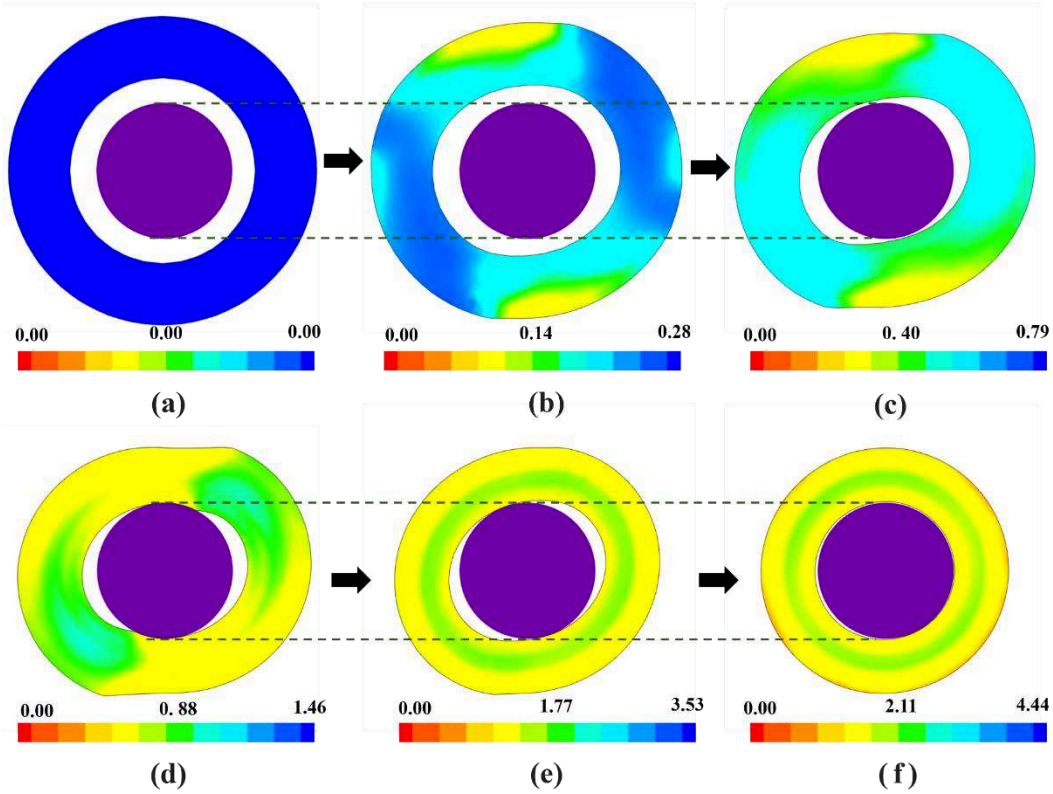

Fig. 14 Formation of the FCWR hole (with strain distribution): (a) initial status; (b) begin of workpiece flattening; (c) begin of mandrel contacting; (d) begin of hole sizing; (e) middle of hole sizing; (f) end of hole sizing

Because mandrel diameter d_m is only 0.73 times of billet hole diameter d_0 as mentioned in Table 3, the mandrel is away from the inner hole and out of work at the initial stage. However, as rolling process goes on, the inner hole becomes elliptical and then workpiece is beginning to contact the mandrel. Latterly, under the double action of mandrel and rollers, the ovality of inner hole becomes small and small and finally growth into round.

The strain distribution of the workpiece is also obtained in Fig. 14. Initially, the billet has local strain at the contacting zone with a small value. But at the hole sizing stage, both the outer and inner of billet undergo a large strain with a value approximate 1.7, which have demonstrated an important advantage of FCWR with mandrel – the wall of workpiece is rolled by external roller and internal mandrel that the properties of rolled wall can be improved effectively.

5 Experiments of FCWR with single guide

5.1 Rolling experiments

The experiments of FCWR hollow shafts with single guide were performed at University of Science and Technology Beijing in the new type of horizontal mill. Experimental tools consisted of two FCWR rollers, several mandrels and one guide as shown in Fig. 15.

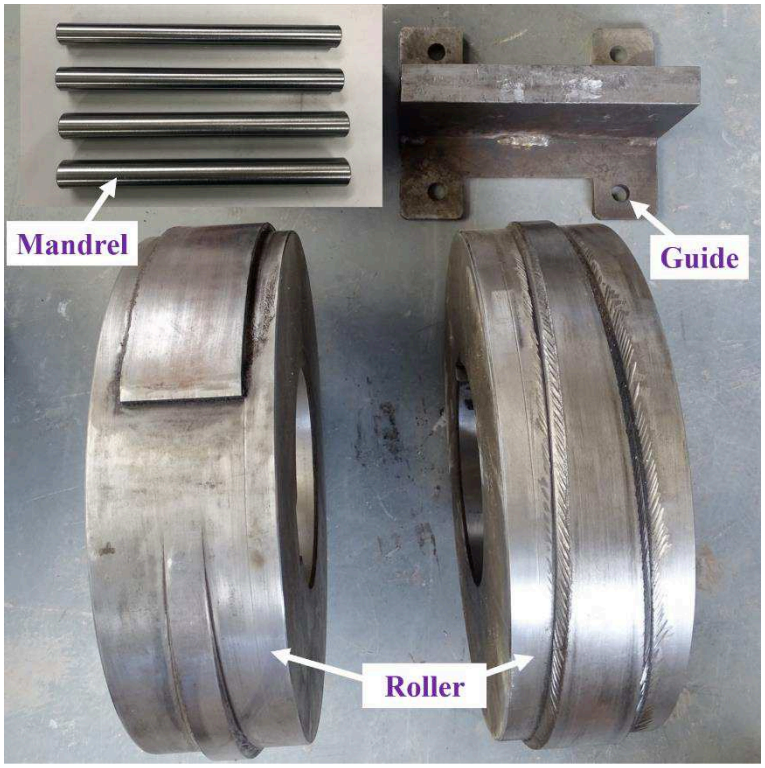

Fig. 15 Tools for FCWR experiments with single guide for hollow shafts

The process parameters of physical experiments corresponded to those of numerical simulations as shown in Tab.3. The guide was mounted between two rollers and downwardly offset from roller centre line with a 28 mm distance.

The rolling experiments was conducted as Fig. 16 shows. Prior to the rolling, the billet was preheated to 1050 ℃ in an electric tube furnace and then immediately transferred to the mill. During the rolling stage, the billet was rotated and deformed under the action of rotating wedges of rollers. After the rolling, the rolled product laid on the top of the guide and then hollow shaft was gained.

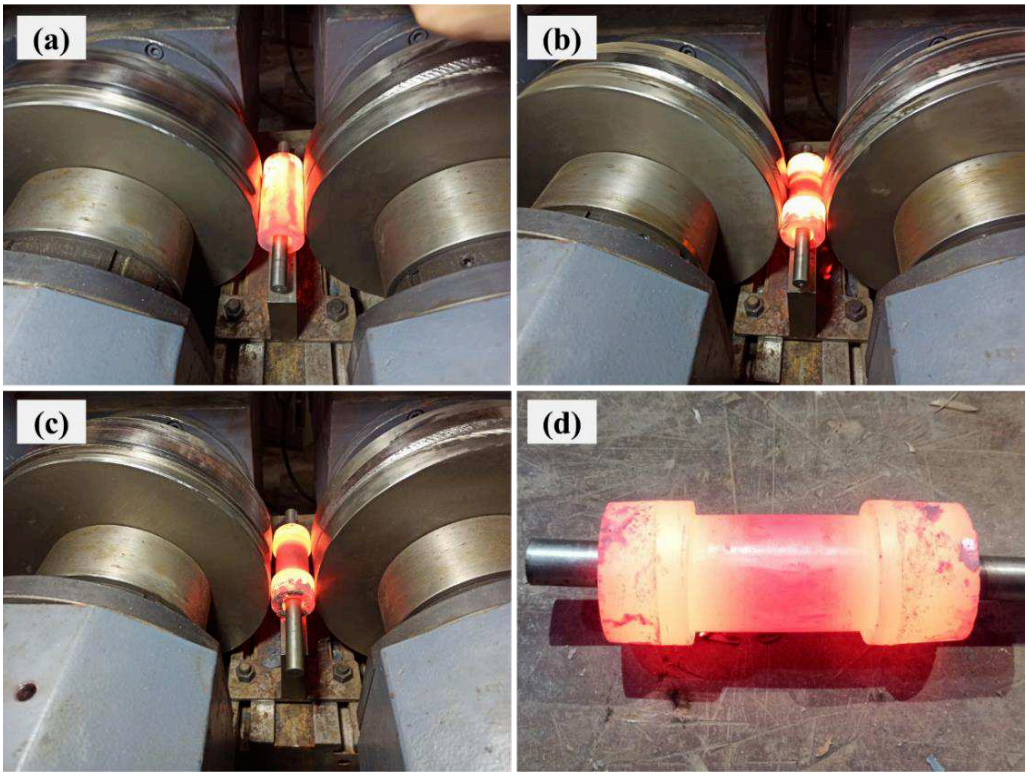

433 **Fig. 16** FCWR rolling experiments in horizontal multifunctional mill with single
434 guide: (a) beginning; (b) rolling stage; (c) ending stage; (d) rolled hollow shaft

435 By the FCWR tests, it can be observed that the workpiece was rolled stably, which
436 has verified the feasibility of the FCWR process and new horizontal multifunctional
437 mill. The produced hollow axles of FCWR rolling tests were cut and shown in Fig. 17a,
438 and its shot peening produts are shown in Fig. 17b. These hollow shafts are free from
439 the typical defects of hole expansion and knifing groove. However, it raises a new
440 question that the rolled shaft cannot be automatically ejected from the mill that a manual
441 transfer is needed.

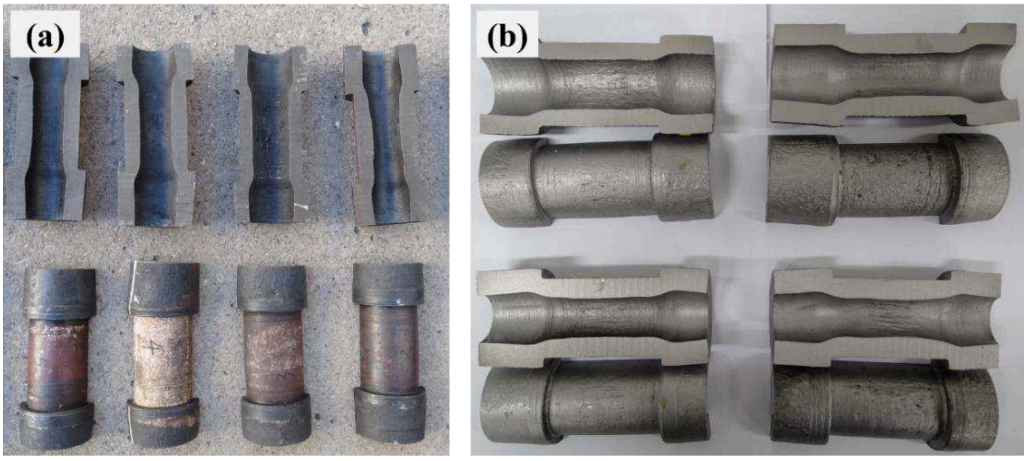

442 **Fig. 17** The FCWR produced hollow shafts: (a) initial status; (b) after shot peening

5.3 Results and Discussion

5.3.1 Validating of the FEM results

A verification method of geometric comparison is employed in this study. The geometries of inner holes are compared to verify the FEM results in consideration of its shapes are related to the flow behavior of material, rolling temperature, friction state and so on. Two groups of experiments including without and with mandrel are compared in Fig.18.

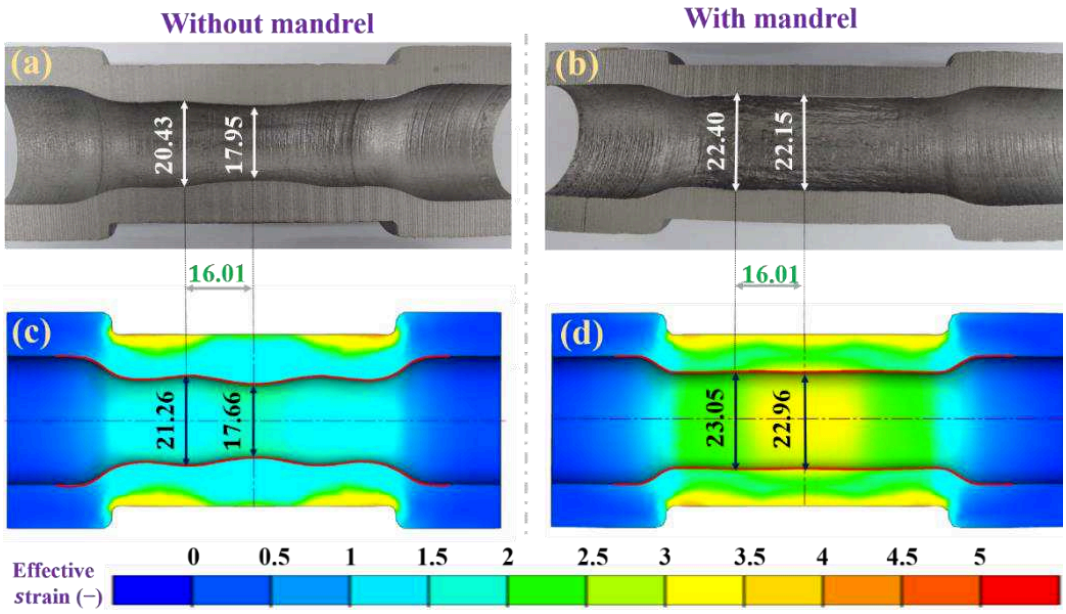

Fig. 18 Geometry comparison between (a, b) physical experiments and (c, d) numerical simulations

The shape of rolled shafts of experimental tests have a good agreement with FE results. In the rolling process without mandrel, both physical and FE shafts have a defect of hole shrinkage on knifing position. But under the circumstance of having a mandrel, this defect is improved and both physical and FE shafts have a uniformed inner diameter.

The maximum and minimum diameters of inner holes are used for quantitative verification. The minimum inner hole diameter of FCWR without mandrel appears on the knifing position with a value equal to 17.95 mm of physical shaft and 17.66 mm of FE result, and its maximum hole diameter is equal to 20.43 mm in physical test and

21.26 mm in FE result. The maximum relative deviation (relative to physical result) of four comparative diameters is 4% which lower than 10%, so the FE results are reliable.

5.3.2 Advantages and disadvantages

Beside the validation experiments, some deformation tests were carried out with varied values of hole diameters. Simultaneously, the mandrel diameters were changed accordingly as dm/d_0 =0.73. The other process parameters stayed the same as D_0=50 mm, α=45 °, β=2 °, h=6 mm, B=18 mm and T=1050 °C. The rolled shafts are presented in Fig. 19.

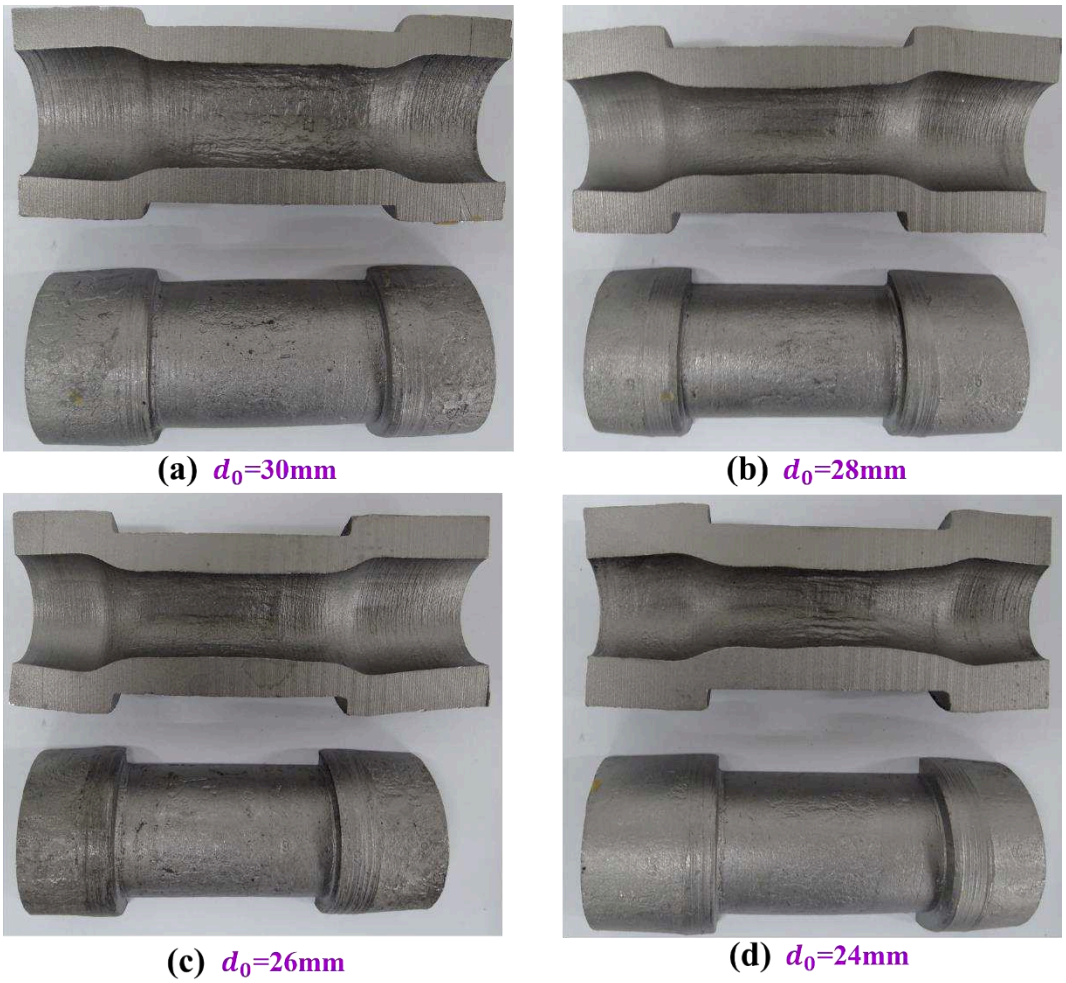

Fig. 19 Hollow shafts formed by FCWR with single guide in the horizontal multifunctional mill

By observing the geometric appearances, we can find that all the rolled pieces are free from knifing groove and hole expansion. Therefore, a conclusion can be gained that the new process can absolutely avoid the forming defects of knifing groove and

hole expansion.

Moreover, these hollow shafts have a good forming accuracy. For example, the right-angle steps are precisely rolled and the typical limitations are absent, such as sprial-grooved surface [15, 18], ellipse of formed shafts [19, 20]. These experimental performances indicate that single guide rolling can improve rolling stability.

The grain size of rolled part is one of the most significant indicators, which decides the mechanical properties of the hollow products. The microstructure morphology of the rolled shaft is obtained in a microscope with 200 times magnification. As Fig. 20 shows, the grain sizes of the rolled regions (P1, P2) are significantly smaller than that of unrolled region (P3), which can be explained that the grains are refined under FCWR deformation. Besides, the grain size at the knifing position (P1) is smaller than that at the stretching position (P2), which is consistent with the distribution of strain shown in Fig.18d, and can be considered that the knifing zone has a larger deformation than the stretching zone.

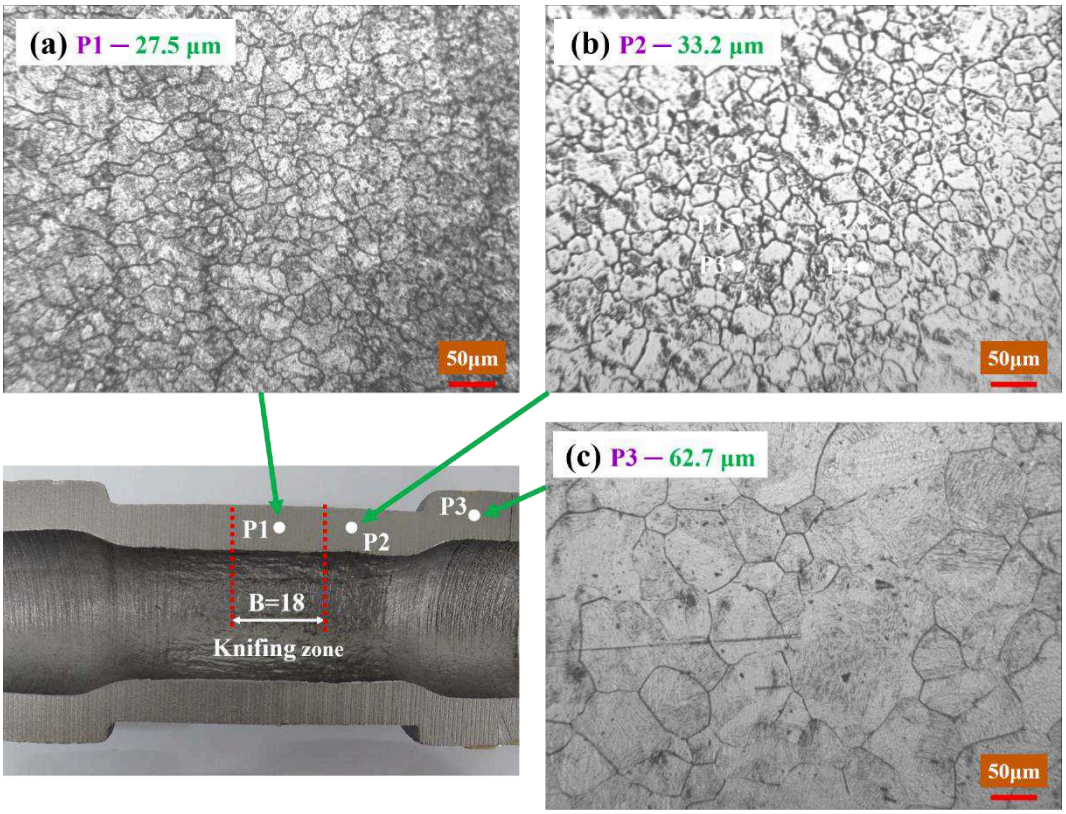

Fig. 20 Grain size of the FCWR rolled shaft at different locations

Although this new process has the above advantages, there are some disadvantages

as well. As arisen in the numerical simulations and physical experiments, the rolled shaft cannot be automatically ejected from the mill so a new discharging device is needed. Besides, FCWR process deteriorates the ellipse of hole and increases rolling force and rotating torque.

5.3.3 Application to the solid shafts

For solid shafts, the FCWR advantage of avoiding hole expansion is no longer necessary. However, it also takes advantages of avoiding knifing groove and reducing the perimeter of rollers.

The major considerations for solid shafts rolling are whether billet can rotate normally and whether central cracks can be avoided. On the one hand, because an BB section (shown in Fig. 10b) is added at the knifing zone, the friction conditions at knifing stage are improved theoretically owing to the contacting area increases. On the other hand, the trend of central cracking is relieved because the added radial compression-force is beneficial to metal bonding. And when it comes to stretching and sizing stage, the deformation of NCWR and FCWR is the same. Therefore, it can be estimated that this novel FCWR process can be used for solid shafts under the condition of reasonable knifing width.

6 Summary and conclusions

In this paper, a novel process of flat-knifing cross-wedge rolling (FCWR) with single guide was proposed to manufacture hollow shafts, including a CWR roller, single guide rolling and a horizontal multifunctional mill. The following conclusions are obtained:

(1) The defects of hole expansion and knifing groove are absolutely avoided because FCWR roller produces a radial force to shrink the hole and avoids the deformation concentration of outer surface during knifing stage;

(2) The new type of horizontal multifunctional mill can be used to perform laboratory tests such as longitudinal rolling, cross rolling and helical rolling and

expected to have industrial application as thread rolling mill, ball rolling mill and cross-wedge rolling mill;

(3) The single guide rolling can be realized by workpiece axis offset from the center line of two rollers, and can improves the rolling stability and simplifies the mill structure;

(4) The flat-knifing roller reduce the wedge length in the range of 200~800 mm;

(5) The process of flat-knifing cross-wedge rolling with single guide brings the shortcomings of non-automatic ejecting, hole ellipse and increasement of rolling force and rotating torque;

(6) The process of FCWR with single guide is estimated to form the solid shafts under the condition that knifing width is designed reasonably.

Compliance with Ethical Standards

Acknowledgments

This work is supported by the National Key R&D Program of China (Grant No. 2018YFB1307900). This work is funded by the National Natural Science Foundation of China (Grant No. 51875036).

Conflict of interest statement

We declare that we have no financial and personal relationships with other people or organizations that can inappropriately influence our work, there is no professional or other personal interest of any nature or kind in any product, service and/or company that could be construed as influencing the position presented in, or the review of, the manuscript entitled.

Ethical approval

This article does not contain any studies with human participants or animals performed by any of the authors.

Informed consent

All the authors listed have approved the manuscript that is enclosed.

Authors' contributions

Longfei Lin: Software, Validation, Methodology, Writing-Original Draft. Baoyu Wang: Project administration, Supervision, Funding acquisition. Jinxia Shen: Methodology, Writing-Reviewing & Editing. Tao Liu: Investigation, Data Curation, Writing-Reviewing & Editing.

Availability of data and materials

The datasets generated and/or analysed during the current study are available from the corresponding author on reasonable request.

Consent to participate

Applicable.

Consent to publish

Applicable.

References

[1] Romanenko V, Stepanov P, Kriskovich S (2018) Production of hollow railroad axles by screw piercing and radial forging. Metallurgist. 61:873-877. https://doi.org/10.1007/s11015-018-0579-0

[2] Ji H, Liu J, Wang B, et al (2017) A new method for manufacturing hollow valves via cross wedge rolling and forging: Numerical analysis and experiment validation. J. Mater. Process. Technol. 240:1-11. https://doi.org/10.1016/j.jmatprotec.2016.09.004

[3] Yang C, Ma J, Hu Z (2017) Analysis and design of cross wedge rolling hollow axle sleeve with mandrel. J. Mater. Process. Technol 239:346-358. https://doi.org/10.1016/j.jmatprotec.2016.09.002

[4] Hu, Z, Wang, B, Zheng Z (2018) Research and industrialization of near-net rolling technology used in shaft parts. Front. Mech. Eng 13:17-24. https://doi.org/10.1007/s11465-018-0480-3

[5] Pater Z, Tofil A (2017) Overview of the research on roll forging processes. Advances in Science and Technology Research Journal 11(2):72-86. https://doi.org/10.12913/22998624/70645

[6] Huo Y, Lin J, Bai Q, Wang B, Tang X, Ji H (2017) Prediction of microstructure and ductile damage of a high-speed railway axle steel during cross wedge rolling. J. Mater. Process. Technol 239:359-369. https://doi.org/10.1016/j.jmatprotec.2016.09.001

[7] Pater Z, Tomczak J, et al (2021) Conception of a three roll cross rolling process of hollow rail axles. ISIJ International 61(3):895–901. https://doi.org/10.2355/isijinternational.ISIJINT-2020-530

[8] Peng W, Zheng S, Chiu Y, Shu X, Zhan L (2016) Multi-wedge cross wedge rolling process of 42CrMo4 large and long hollow shaft. Rare Metal Materials and Engineering 45(4): 836-842. https://doi.org/10.1016/S1875-5372(16)30084-4

[9] Bartnicki J, Pater Z (2004) The aspects of stability in cross-wedge rolling processes of hollowed shafts. J. Mater. Process. Technol 155-156:1867-1873. https://doi.org/10.1016/j.jmatprotec.2004.04.278

[10] Bartnicki J, Pater Z (2005) Numerical simulation of three-rolls cross-wedge rolling of hollowed shaft. J. Mater. Process. Technol 164-165:1154-1159. https://doi.org/10.1016/j.jmatprotec.2005.02.120

[11] Urankar S, Lovell M, Morrow C, Li Q, Kawada K (2006) Establishment of failure conditions for the cross-wedge rolling of hollow shafts. J. Mater. Process. Technol 177:545-549. https://doi.org/10.1016/j.jmatprotec.2006.04.052

[12] Neugebauer R, Glass R, Kolbe M (2002) Optimisation of processing routes for cross rolling and spin extrusion. J. Mater. Process. Technol 125:856-862. https://doi.org/10.1016/S0924-0136(02)00392-8

[13] Landgrebe D, Steger J, Böhmichen U, et al (2018) Modified cross-wedge rolling for creating hollow shafts. Procedia Manufacturing 21:53-59. https://doi.org/10.1016/j.promfg.2018.02.094

[14] Shen J, Wang B, Lin L, Li J, Zhu C (2020) Investigation on the hole evolution and forming dimensions during cross wedge rolling hollow shaft with mandrel. Procedia Manufacturing 50:143-147. https://doi.org/10.1016/j.promfg.2020.08.027

[15] Shen J, Wang B, Zhou J, Huang X, Li J (2019) Numerical and experimental research on cross wedge rolling hollow shafts with a variable inner diameter. Arch Civ Mech Eng 4:1497-1510. https://doi.org/10.1016/j.acme.2019.08.003

[16] Shen J, Wang B, et al (2021) Theoretical study and prediction of the inner hole reduction and critical mandrel diameter in cross wedge rolling of hollow shaft. J. Mater. Process. Technol 294(2):117140. https://doi.org/10.1016/j.jmatprotec.2021.117140

[17] Ji H, Liu J, Wang B, et al (2016) Constitutive relationship of 4Cr9Si2 and technological parameters on the inner bore of cross wedge rolling for preform hollow valves. Int. J. Adv. Manuf. Tech 86(9-12):1-13. https://doi.org/10.1007/s00170-016-8360-7

[18] Shu X, Shi J, Chen Ji, Yang H (2021) Effect of process parameters on surface

614 quality of shafts parts formed by warm cross wedge rolling. Int. J. Adv. Manuf.
615 Tech 113:2819-2813. https://doi.org/10.1007/s00170-021-06784-2

616 [19] Huang X, Wang B, et al (2019) Investigation on the effect of mandrels on hollow
617 shafts in cross-wedge rolling. Int. J. Adv. Manuf. Tech 102:443-455.
618 https://doi.org/10.1007/s00170-018-3093-4

619 [20] Feng P, Yang C, Wang B, et al (2021) Formability and microstructure of TC4
620 titanium alloy hollow shafts formed by cross-wedge rolling with a mandrel. Int. J.
621 Adv. Manuf. Tech 114:365–377. https://doi.org/10.1007/s00170-021-06635-0

622 [21] Pater Z. Cross-Wedge Rolling (2014) Comprehensive Materials Processing, Button,
623 S.T, Ed. Elsevier Ltd 3:211-279. https://doi.org/10.1016/B978-0-08-096532-
624 1.00315-0

625 [22] Shu X, Shchukin V, Kozhevnikova G, et al (2004) Theory and technology of cross
626 wedge rolling. Beijing: The Science Publishing Company. ISBN: 978-7-03-
627 040397-1 (**In Chinese**).

628 [23] Wang B, Lin L, Wang S, Yang C, Liu S, Zhang H (2020) Flexible skew rolling mill
629 with dual-rotatable-shafts. United State Patent. No, 20200398323.

630 [24] Huang X, Wang B, et al (2017) Effect of mandrel diameter on non-circularity of
631 hollow shafts in cross wedge rolling. Procedia Eng 207:2376-2381.
632 https://doi.org/10.1016/j.proeng.2017.10.1011

633 [25] Tofil A, Tomczak J, Bulzak T (2015) Numerical and experimental study on
634 producing aluminium alloy 6061 shafts by cross wedge rolling using a universal
635 rolling mill. Arch. Metall. Mater 60(2):801-807. https://doi.org/10.1515/amm-
636 2015-0210

637 [26] Pater Z, Tomczak J, Bulzak T (2016) Cross-wedge rolling of driving shaft from
638 titanium alloy Ti6Al4V. Key Eng Mat 687:125–32.
639 https://doi.org/10.4028/www.scientific.net/KEM.687.125

640 [27] Lis K, Wójcik U, Pater Z (2016) Numerical analysis of a skew rolling process for
641 producing a crankshaft preform. Open Engineering 6:581-584.
642 https://doi.org/10.1515/eng-2016-0087

643 [28] Pater Z, Tomczak J, Lis K, et al (2020) Forming of rail car axles in a CNC skew
644 rolling mill. Arch Civ Mech Eng 20:69-82. https://doi.org/10.1007/s43452-020-
645 00075-5

Figures

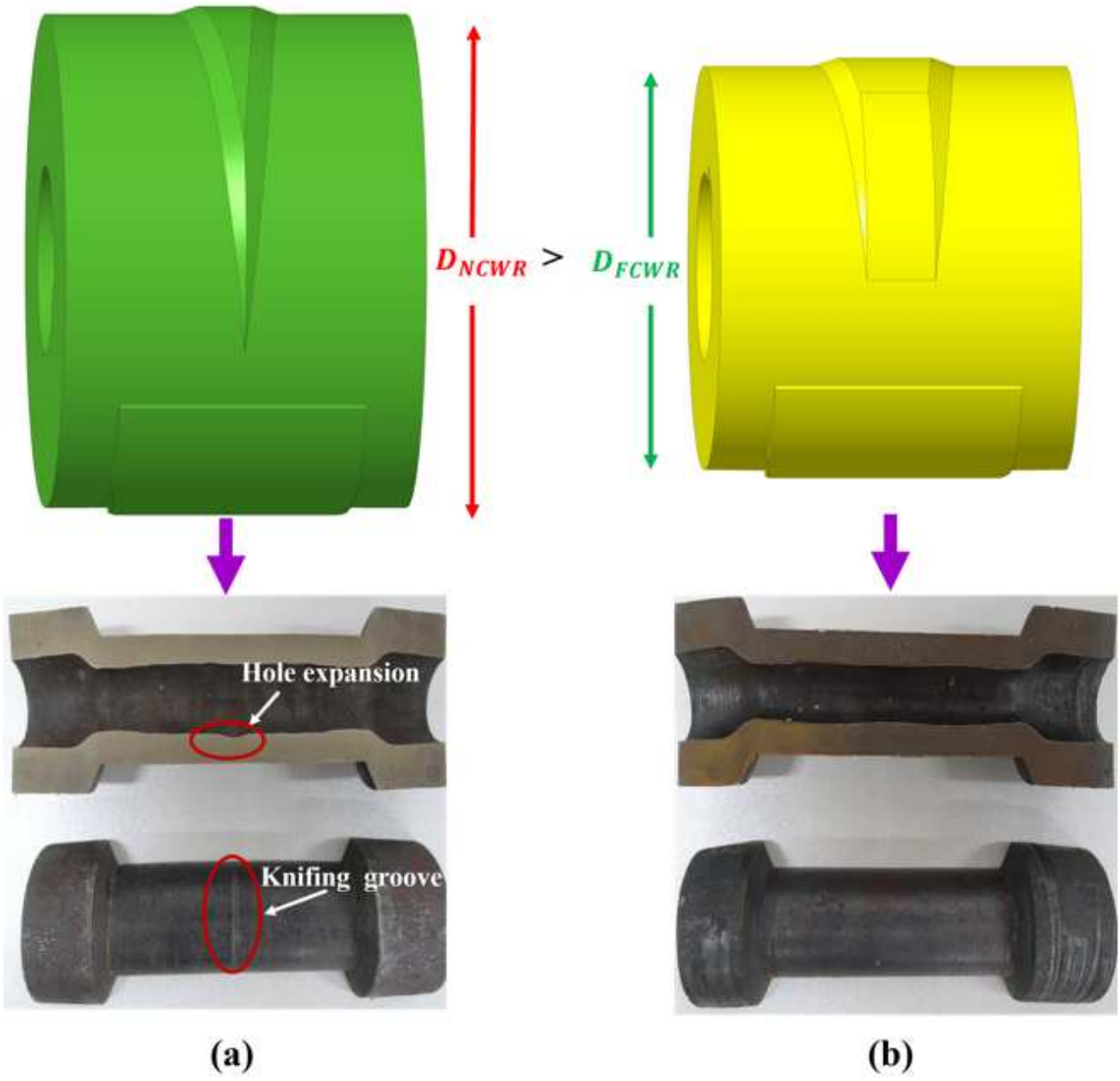

Figure 1

Contrast between two methods for hollow shafts：(a) normalized CWR; (b) flat-knifing CWR

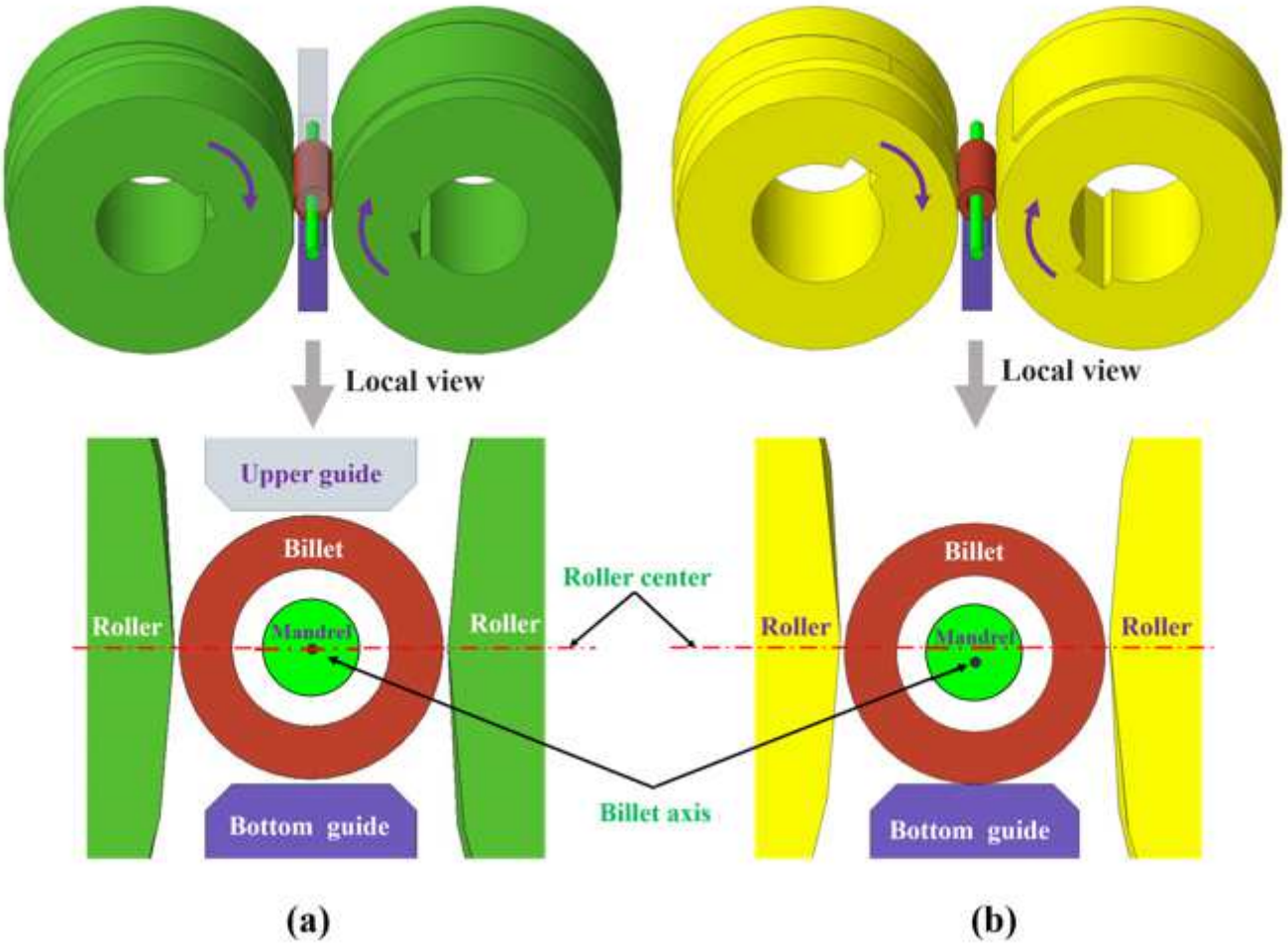

Figure 2

Process principle: (a) NCWR with two guides; (b) FCWR with single guide

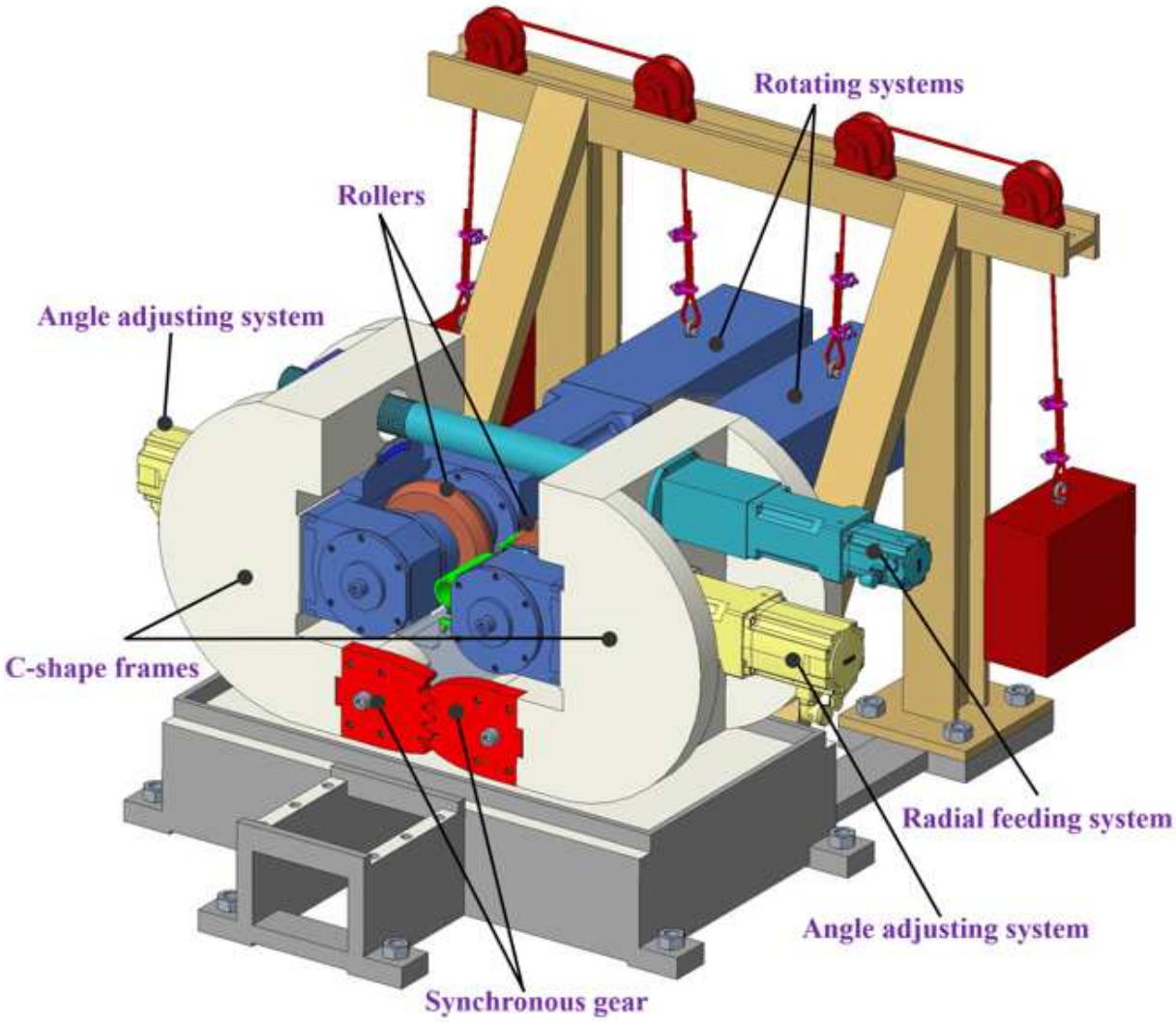

Figure 3

Geometrical model of the horizontal multifunctional mill

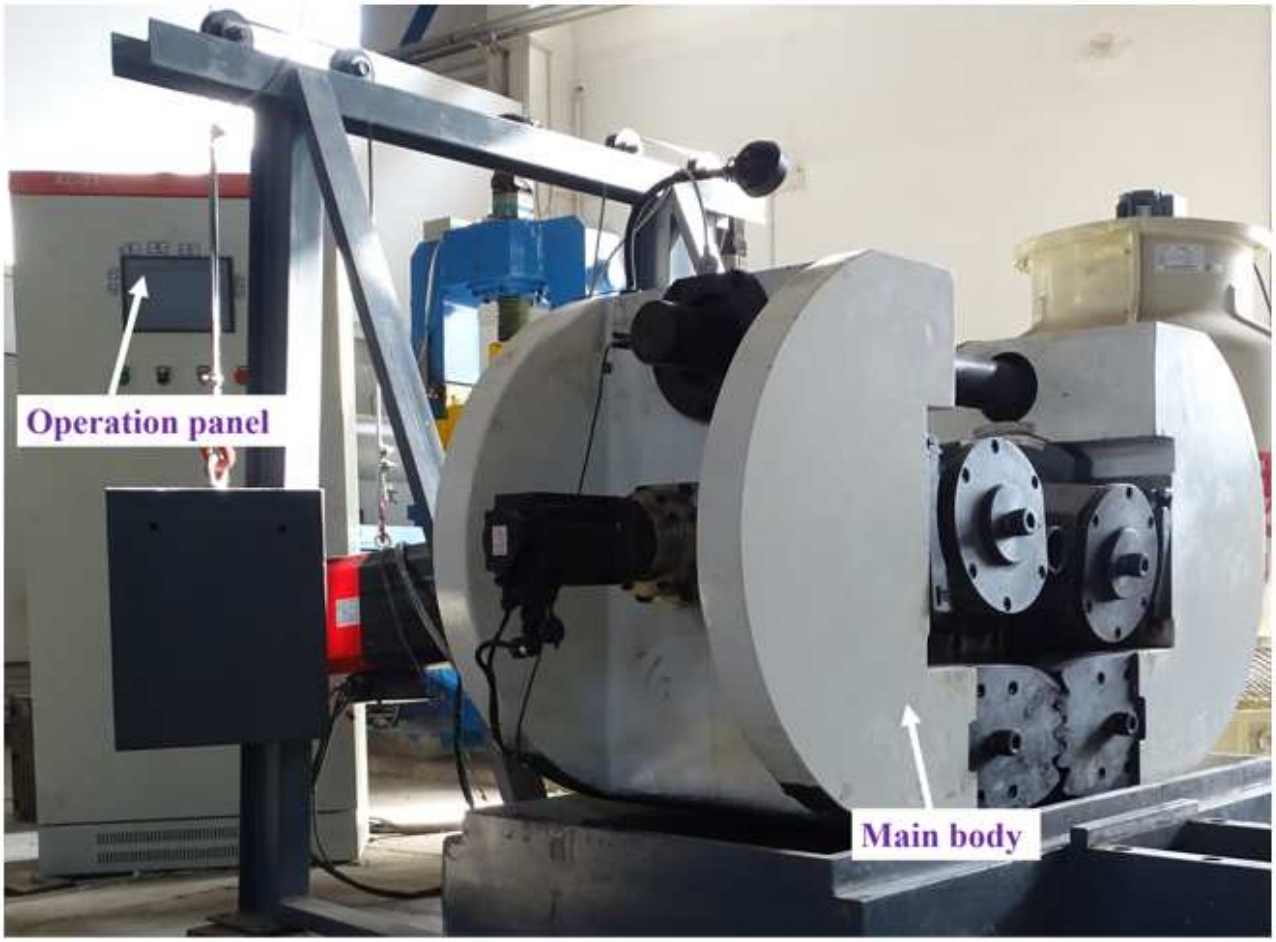

Figure 4

The constructed horizontal multifunctional mill

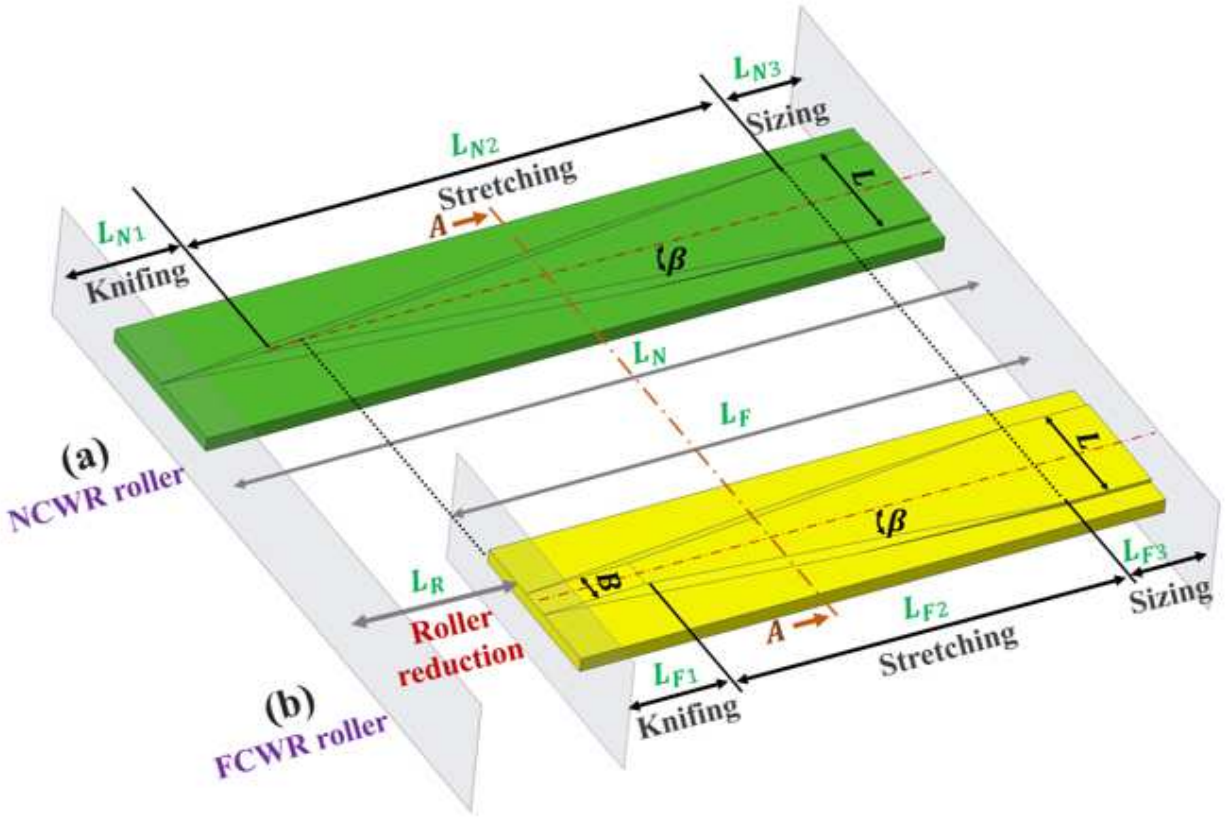

Figure 5

Configuration and major parameters of NCWR and FCWR roller

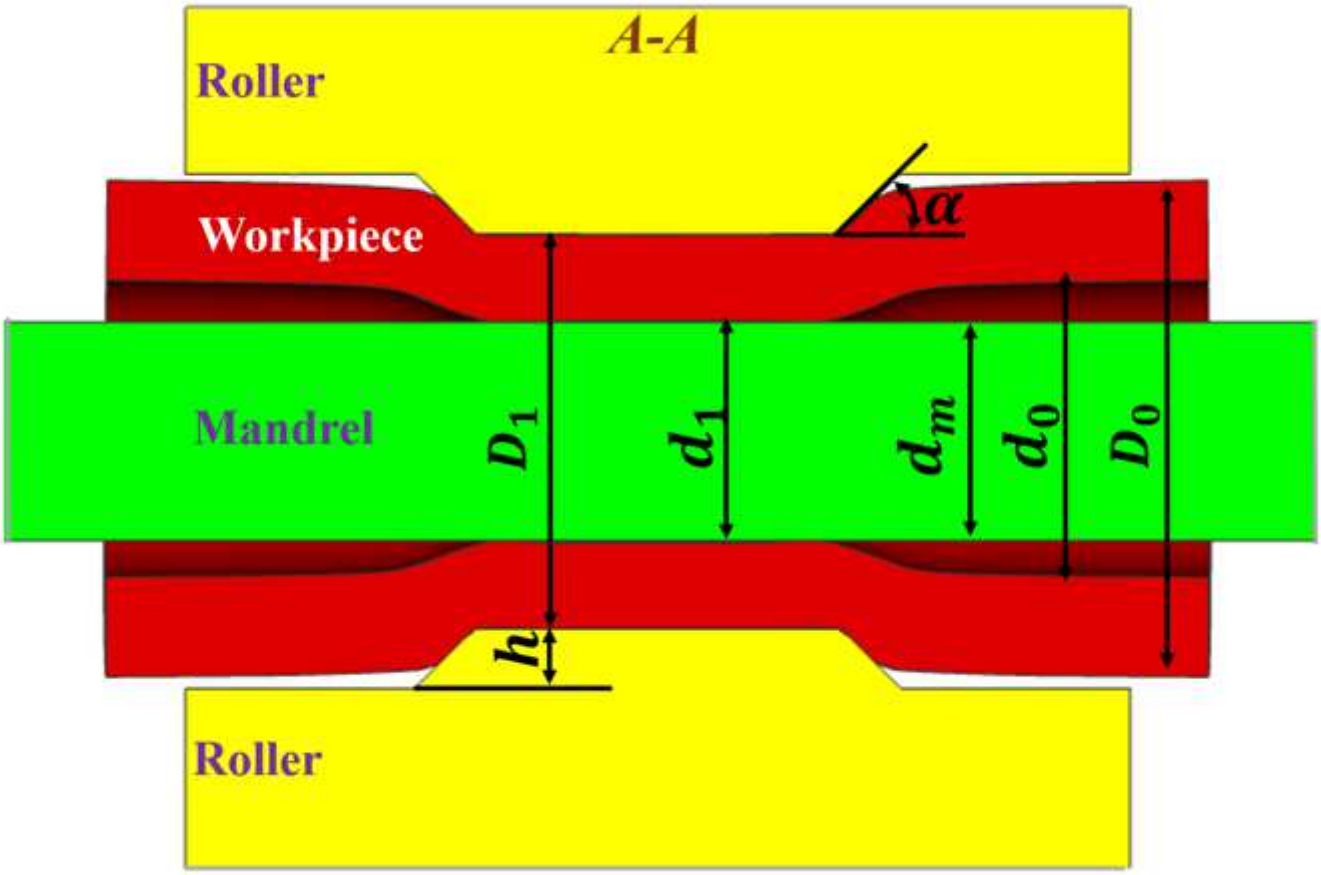

Figure 6

Contact model of roller, mandrel and workpiece at the stretching stage

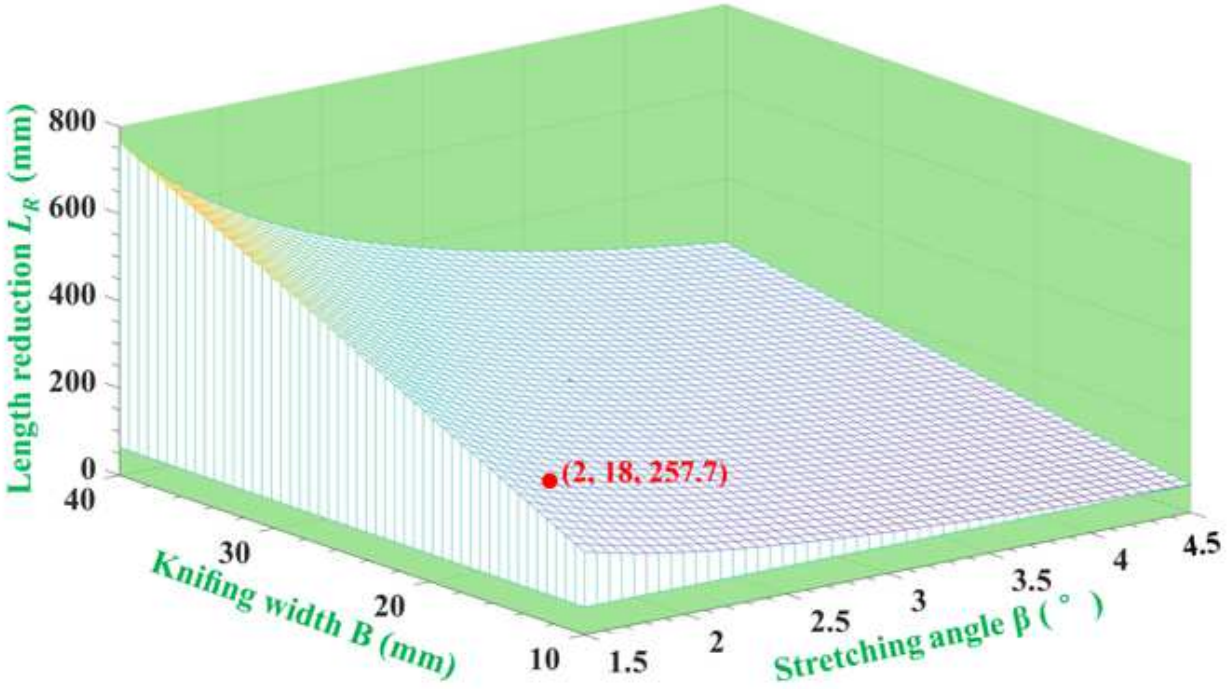

Figure 7

Relationship between wedge-length reduction and process parameters

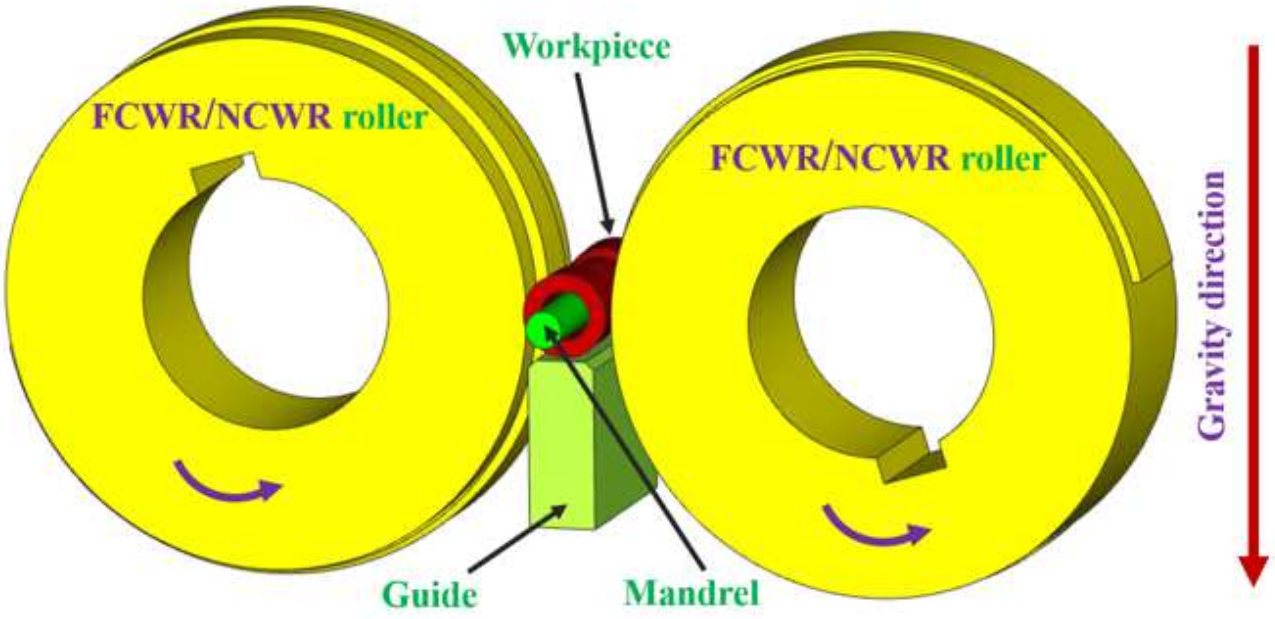

Figure 8

FE projects of FCWR and NCWR with single guide

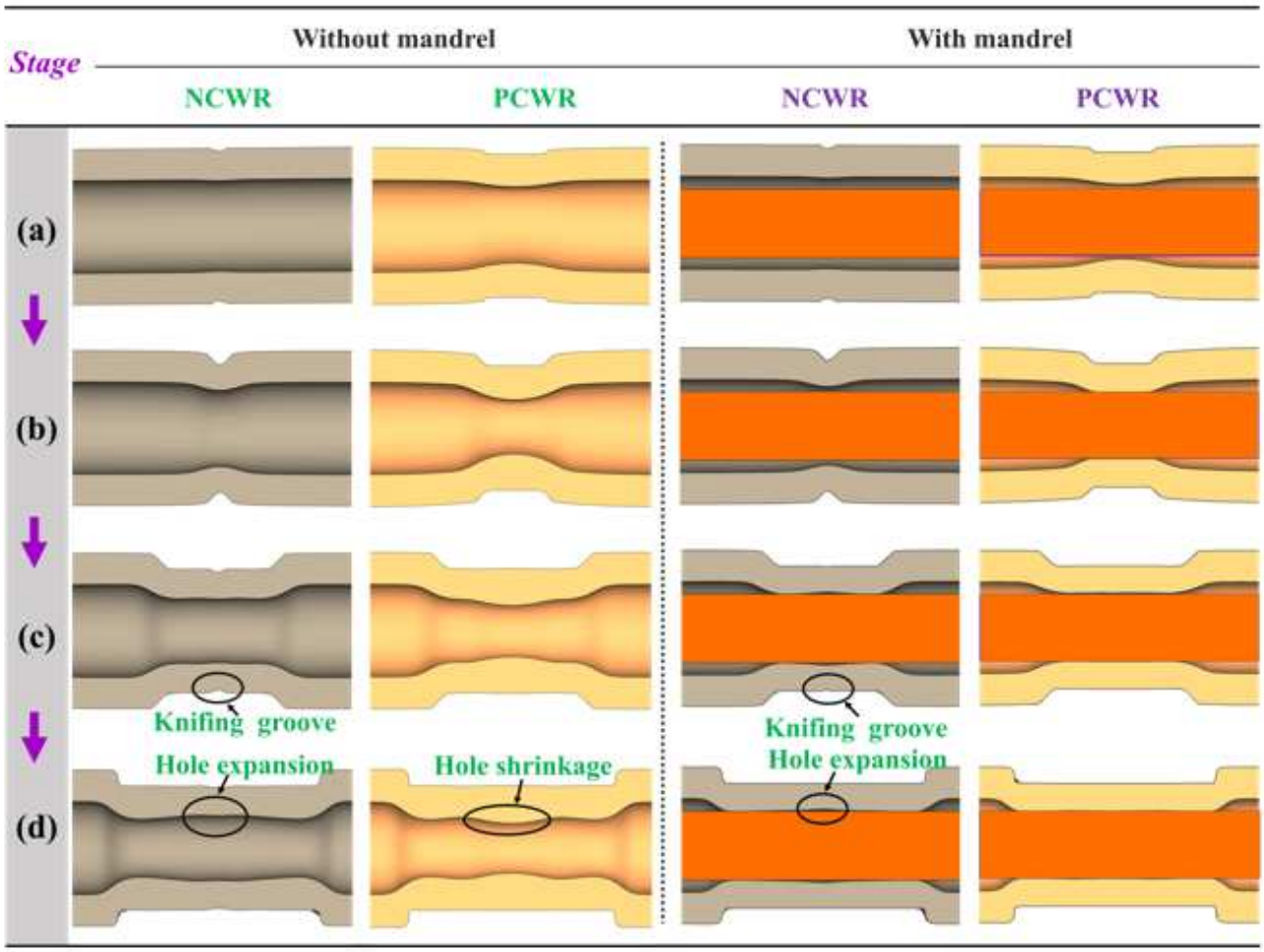

Figure 9

FE results of NCWR and FCWR: (a) middle of knifing stage; (b) end of knifing stage; (c) middle of stretching stage; (d) end of stretching stage

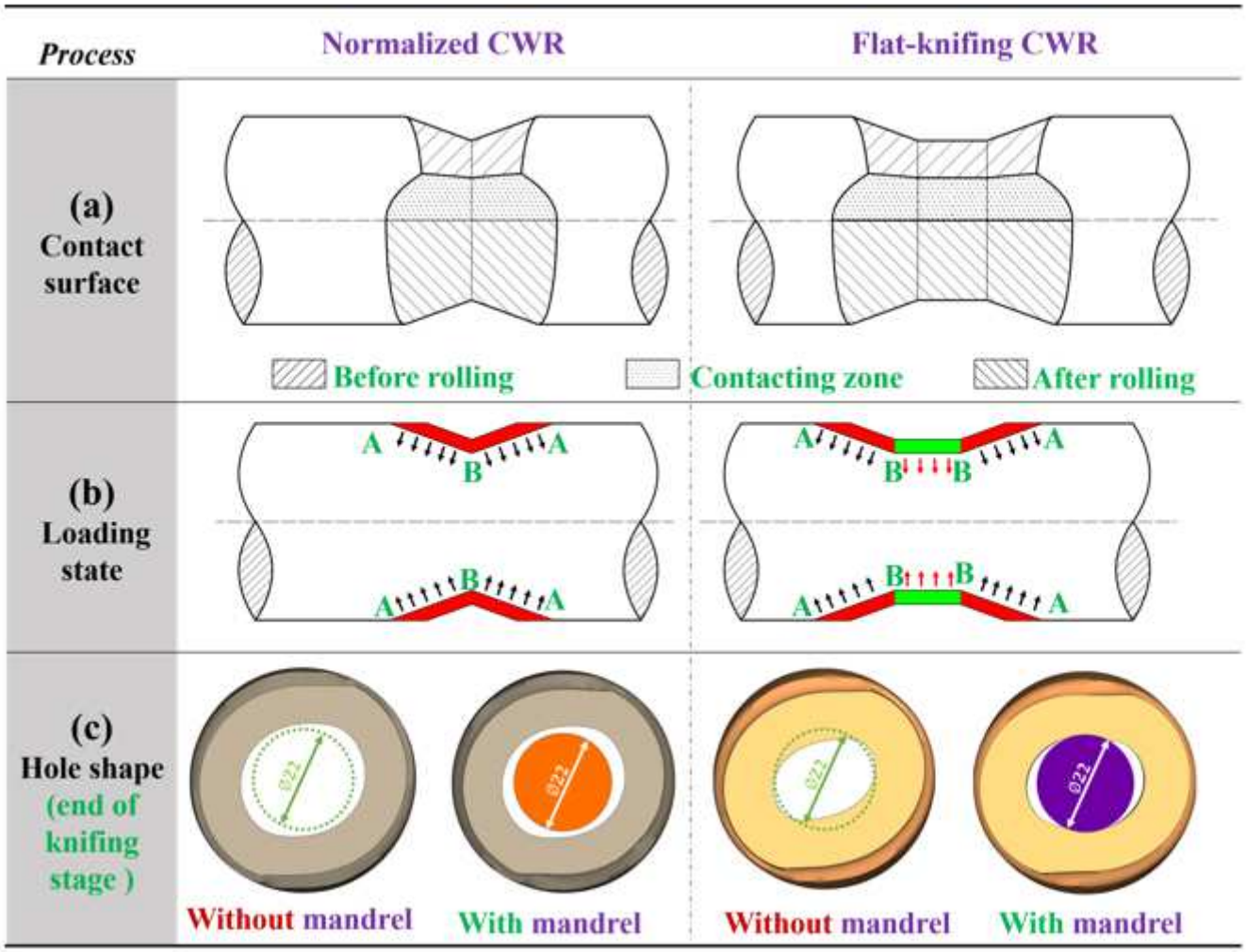

Figure 10

Formation mechanism of hole expansion (end of knifing stage): (a) contact surface; (b) loading states; (c) hole shape

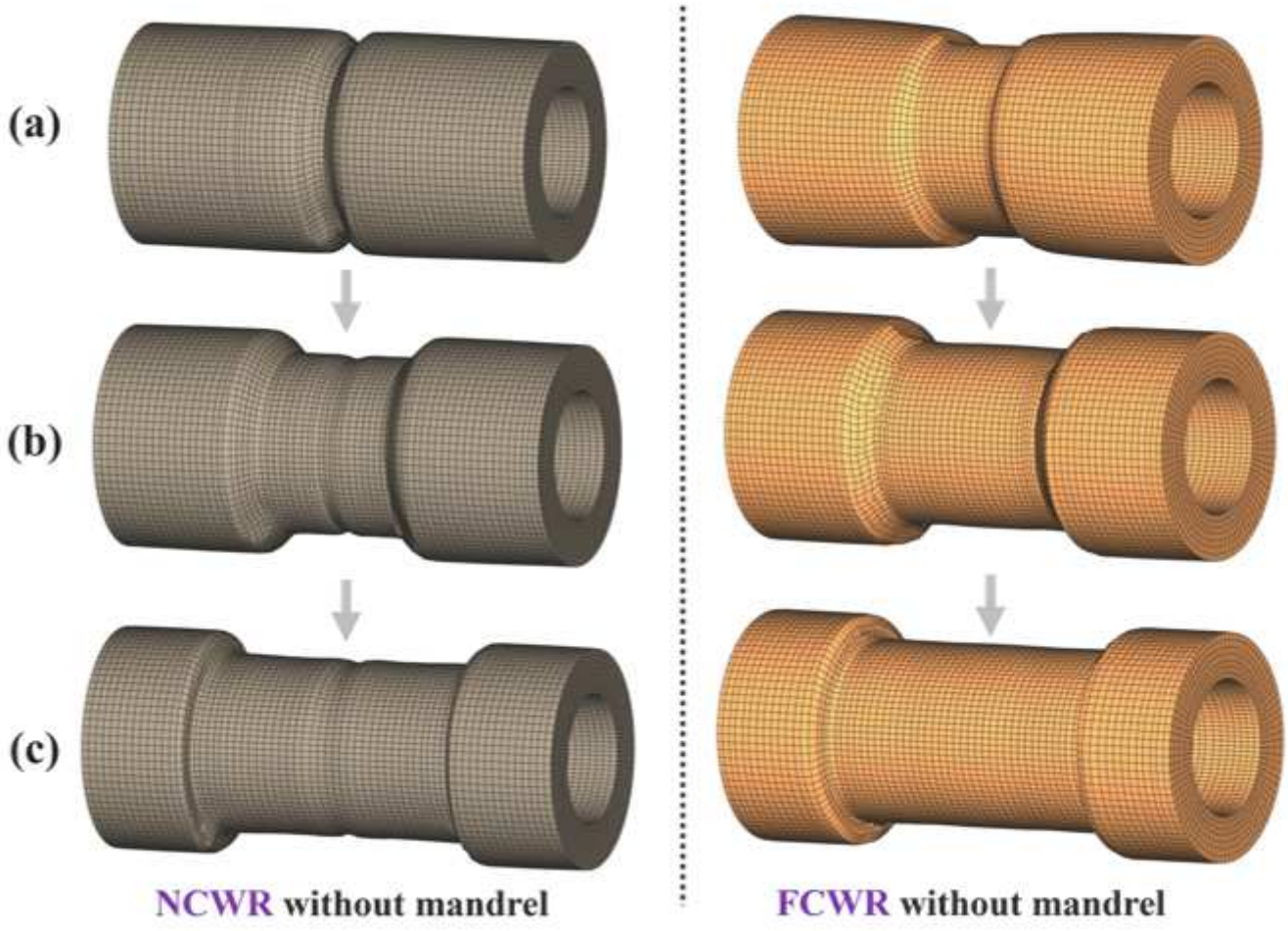

Figure 11

Geometry comparison between NCWR and FCWR workpiece: (a) end of knifing stage; (b) middle of stretching stage; (c) end of stretching stage

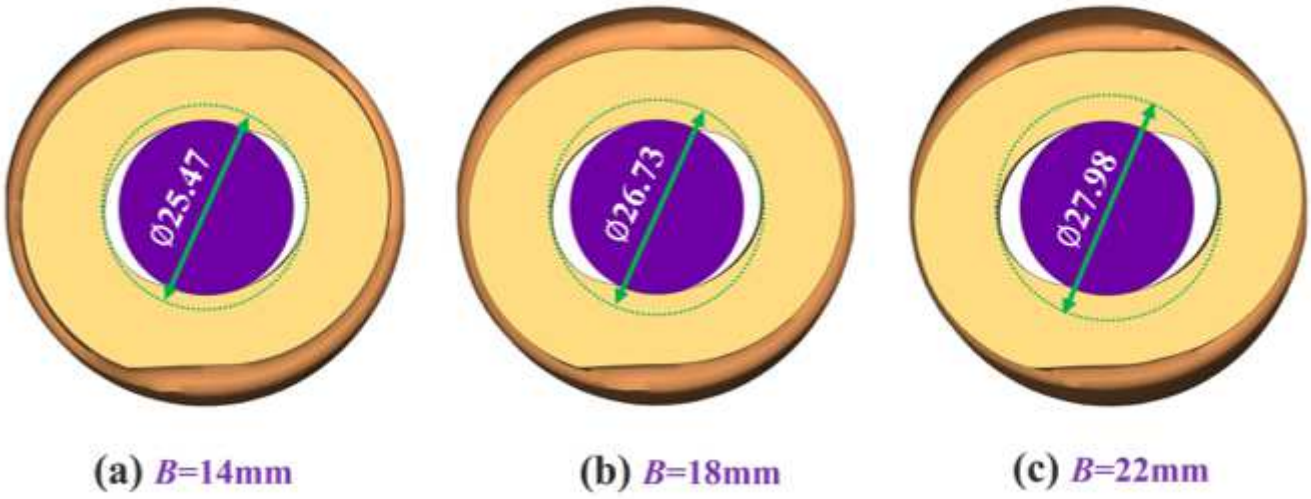

Figure 12

Relationship between knifing width and hole ovality (end of knifing stage)

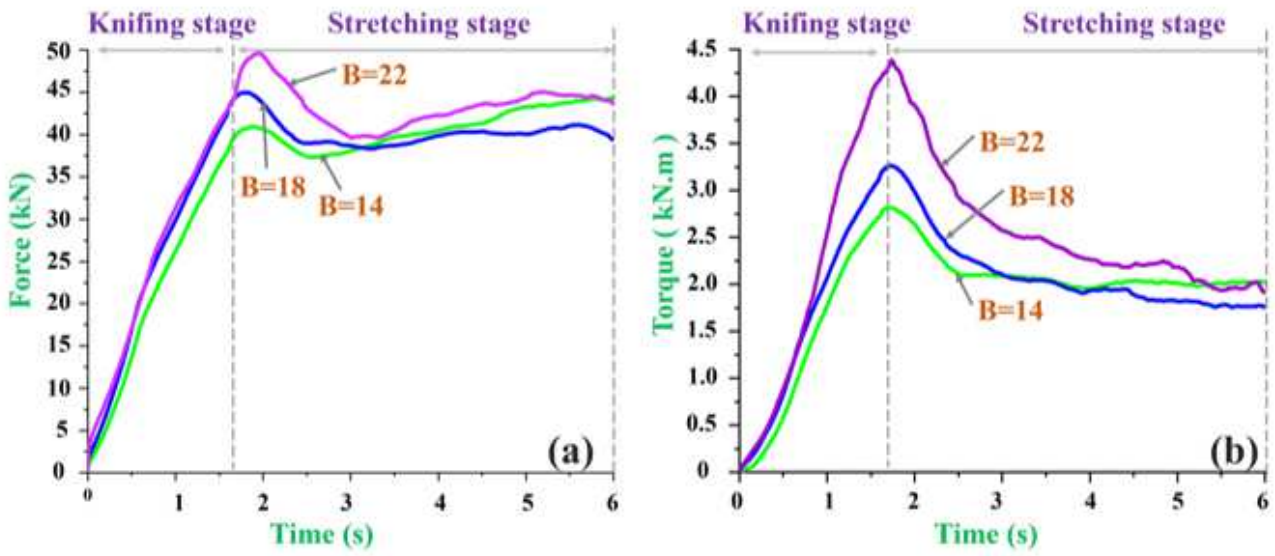

Figure 13

Relationship between knifing width, (a) rolling force, (b) rotating torque

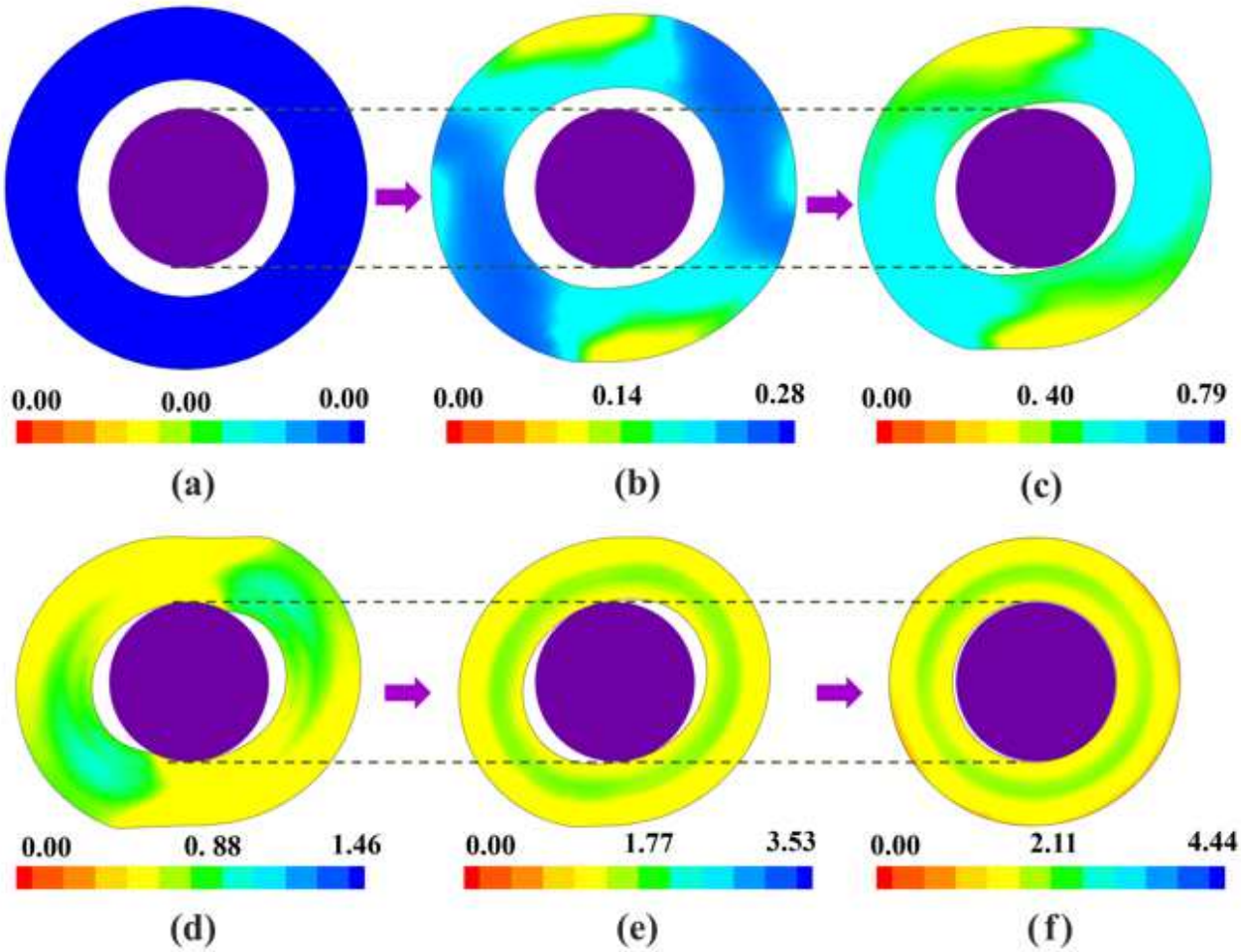

Figure 14

Formation of the FCWR hole (with strain distribution): (a) initial status; (b) begin of workpiece flattening; (c) begin of mandrel contacting; (d) begin of hole sizing; (e) middle of hole sizing; (f) end of hole sizing

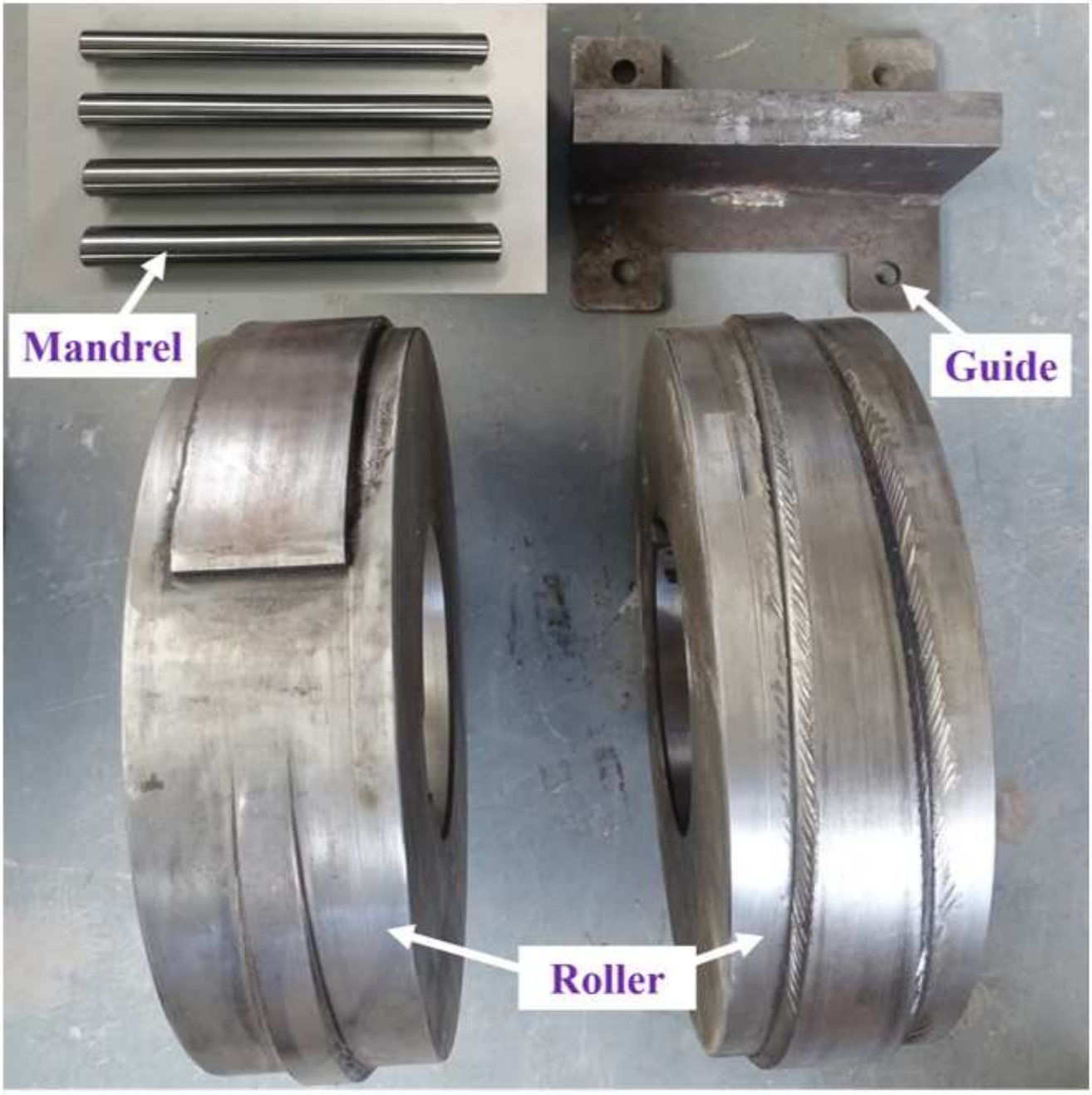

Figure 15

Tools for FCWR experiments with single guide for hollow shafts

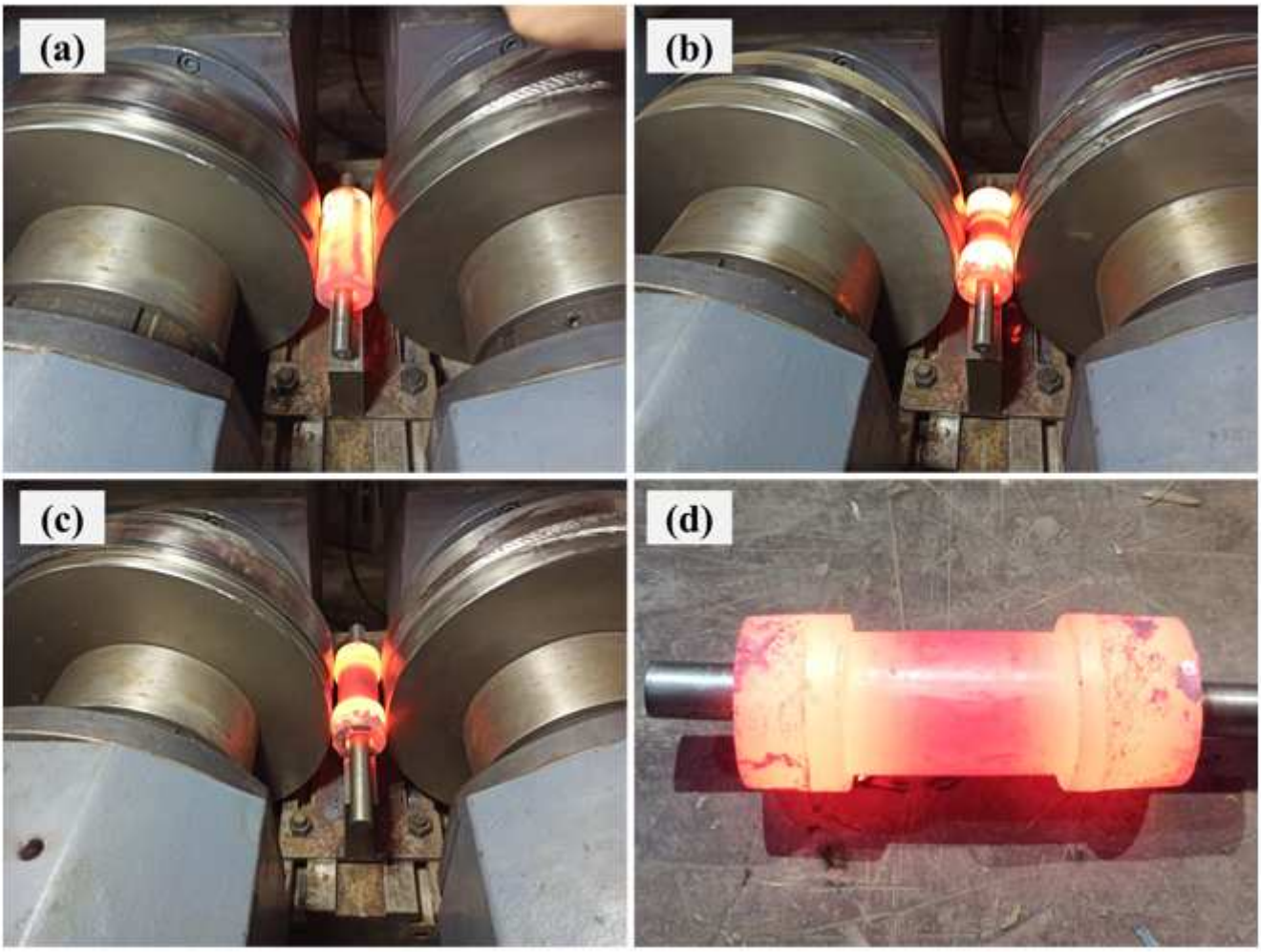

Figure 16

FCWR rolling experiments in horizontal multifunctional mill with single guide: (a) beginning; (b) rolling stage; (c) ending stage; (d) rolled hollow shaft

Figure 17

The FCWR produced hollow shafts: (a) initial status; (b) after shot peening

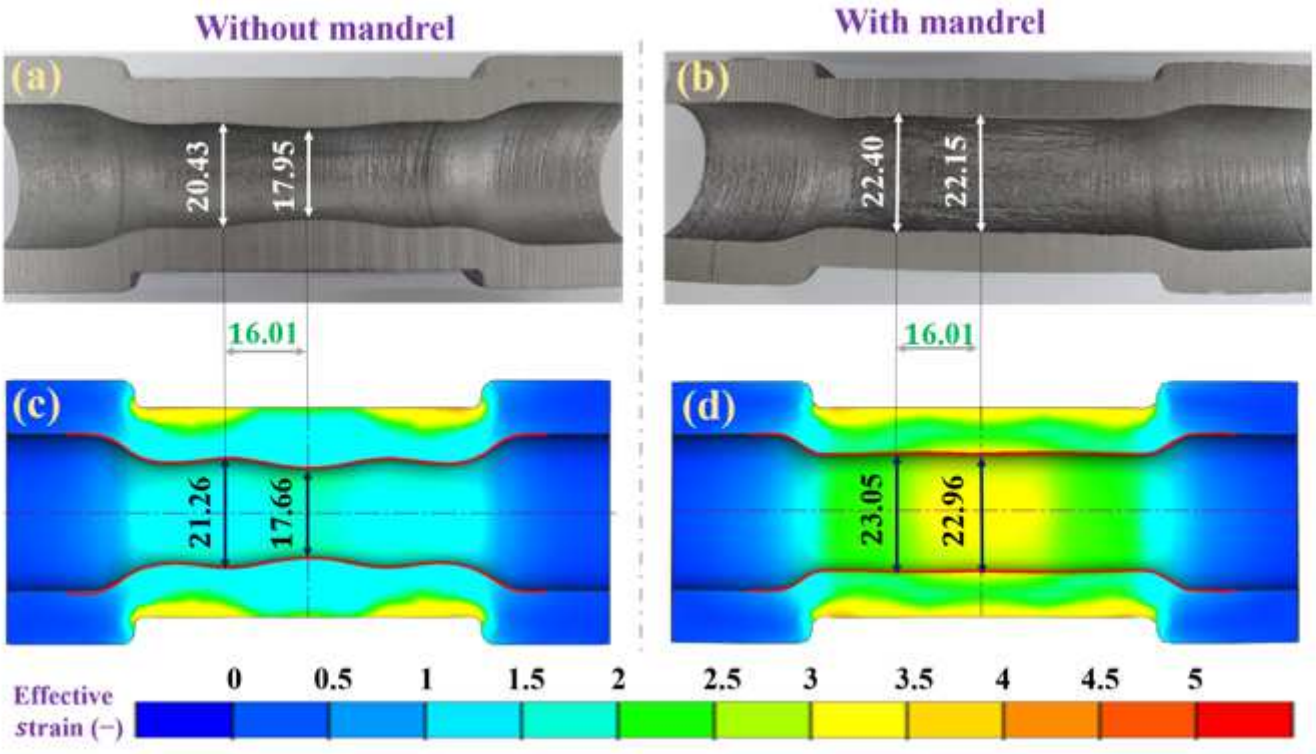

Figure 18

Geometry comparison between (a, b) physical experiments and (c, d) numerical simulations

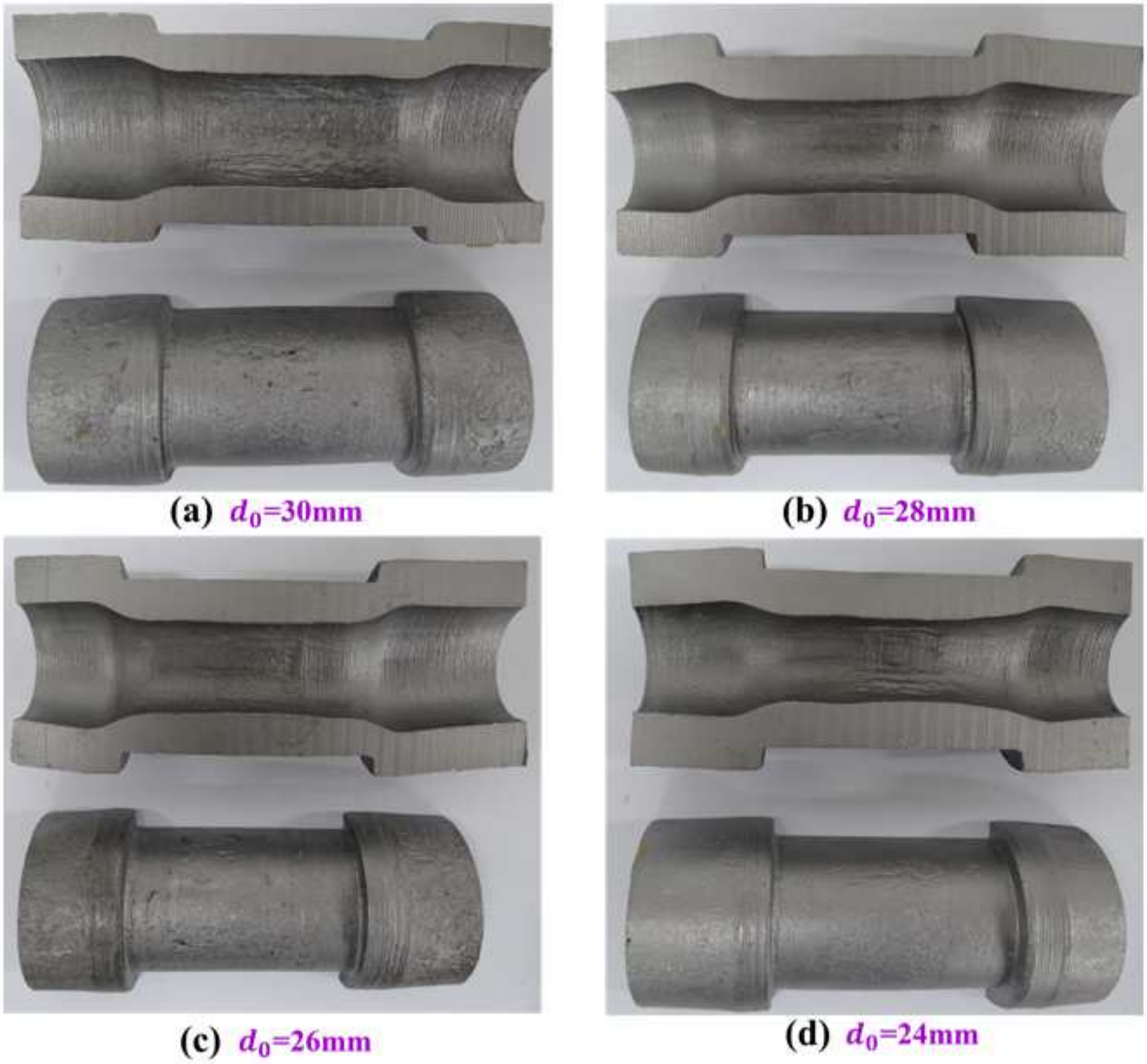

Figure 19

Hollow shafts formed by FCWR with single guide in the horizontal multifunctional mill

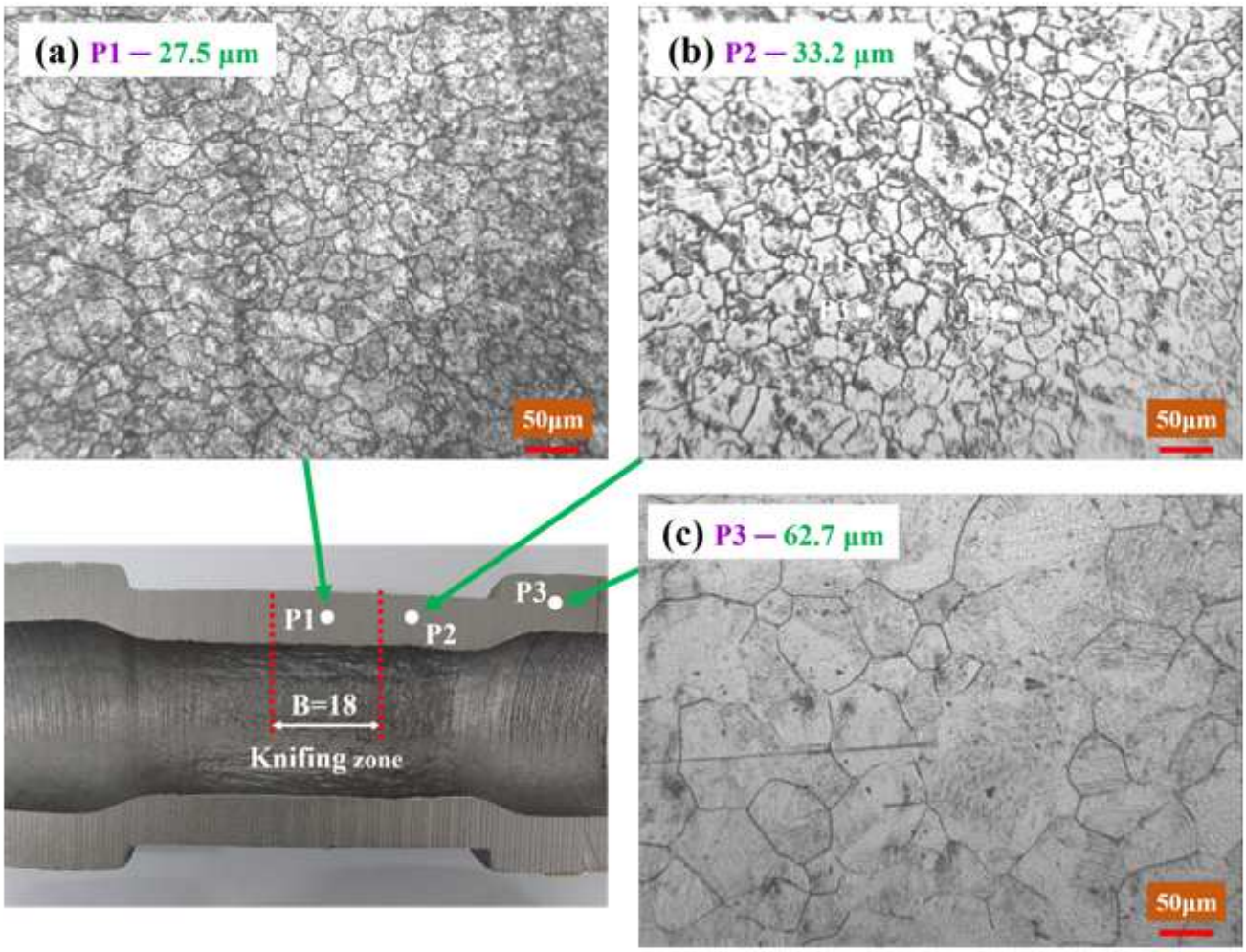

Figure 20

Grain size of the FCWR rolled shaft at different locations